NASA CR-132387

Cyclic-Stress Analysis of Notches for Supersonic Transport Conditions

CONTRACT NAS1-12484

FEBRUARY 8, 1974

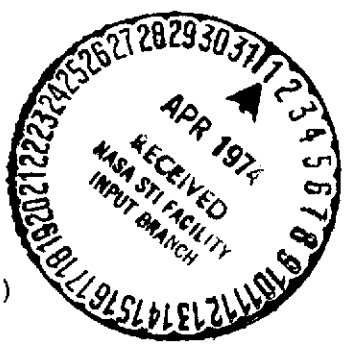

PREPARED BY
BOEING AEROSPACE COMPANY
(A DIVISION OF THE BOEING COMPANY)
RESEARCH AND ENGINEERING
SEATTLE, WASHINGTON

PREPARED FOR
NATIONAL AERONAUTICS AND SPACE ADMINISTRATION
LANGLEY RESEARCH CENTER
HAMPTON, VIRGINIA

CONTENTS

LIST OF FIGURES

LIST OF FIGURES (CONTINUED)

LIST OF TABLES

1.0 SUMMARY

The objective of this study was to demonstrate the feasibility of using the finite-element method to account for the effects of cyclic load and temperature on local stresses and strains at a notch. In particular the study concerns the behavior of a notched titanium panel under variable loads and temperatures representative of flight conditions for the lower wing surface of a Supersonic Transport (SST). The analysis was performed with the use of the BOPACE finite-element computer program which provides capability to determine high temperature and large visco-plastic effects caused by cyclic thermal and mechanical loads. The analysis involves the development of the finite-element model as well as determination of the structural behavior of the notched panel. Results are presented for twelve SST flights comprised of five different load-temperature cycles. The results show the approach is feasible, but material response to cyclic loads, temperatures, and hold times requires improved understanding to allow proper modeling of the material.

BOPACE is the acronym for the BOeing Plastic Analysis Capability for Engines.

THIS PAGE LEFT INTENTIONALLY BLANK.

2.0 INTRODUCTION

The distribution of elastic stress in a structure may be nominally uniform or may vary in some regular manner. When the variation is abrupt the condition is described as stress concentration. Stress concentration is usually the result of local irregularities such as small holes or some other stress raiser.

The maximum values of elastic stresses caused by many kinds of common stress raisers have been the subject of extensive analytical and experimental studies. However, it is for conditions involving inelastic behavior and fatigue that stress concentrations are most important. The classical approach to the solution of such problems has been to measure notch effects by the so-called factor of stress concentration for fatigue K_f. Methods for evaluation of notch effects based on the use of K_f are valuable and applicable with certain limitations, but none can be applied with confidence to all situations. For example, previous efforts were restricted to problems involving constant temperature. These results do not apply to complex problems such as fatigue of SST structure which involves local viscoplastic material behavior as well as variable temperatures at a notch.

A more reliable approach to the solution of the effects of a stress raiser on fatigue is the determination of the history of local stress and strain and the use of these data in a damage assessment. Owing to the complexity of the problem, such solutions are available only through the use of numerical techniques such as the finite-element analysis method. This method, inherent in the BOPACE computer program, provides the capability to solve a large variety of nonlinear problems in viscoplasticity with variable temperatures and loading.

This study is concerned with the formulation and solution of problems in viscoplastic behavior of a notched panel of titanium alloy under

2.0 (Continued)

loads and temperatures representative of SST flight conditions [1, 2, 3]. Finite-element models are developed and are analyzed with the BOPACE program. A discussion of certain constitutive assumptions necessary for modeling the panel material is also given. Numerical results in the form of stress-strain hysteresis loops and stress variations are provided and discussed in light of the constitutive assumptions.

3.0 PROBLEM DEFINITION

The structure of an SST, like that of conventional aircraft, will contain many holes which are stress raisers. Fatigue failures which generally originate from the most critical stress raisers can be predicted if the local stress-strain histories are determined for loads and temperatures imposed during airplane operation. The aerodynamic heating experienced by SST structures complicates the analysis by altering material properties, causing increased local plasticity, and inducing creep or relaxation under sustained load or deformation. The finite-element method appears to be the only suitable approach to numerical solution of such problems, and the BOPACE program was used to account for variable-amplitude cyclic loads, variable temperature effects on material properties, and mechanically and thermally induced elastic and viscoplastic deformations.

3.1 NOTCHED PANEL CONFIGURATION AND MATERIAL PROPERTIES

The structure analyzed during this study consisted of a notched uniaxial test panel of Ti-6Al-4V duplex-annealed titanium alloy. The specimen configuration, shown in Figure 3.1-1, represents a region of a SST lower wing panel containing a moderate stress concentration.

Typical material properties which characterize temperature effects on Ti-6Al-4V are shown in Figures 3.1-2, 3.1-3, 3.1-4 and 3.1-5. These material properties were provided by the National Aeronautics and Space Administration (NASA) for this study. Figure 3.1-2 presents the tensile portion of uniaxial stress-strain curves for cyclically stabilized Ti-6Al-4V at 297.0°K and 560.9°K. Figure 3.1-3 shows the variation in Young's modulus for the same temperature range. Figures 3.1-4 and 3.1-5 show creep curves. The creep data indicate zero creep at stresses below 862 N/mm^2 and 620 N/mm^2 at 297.0°K and 560.9°K respectively.

3.2 THERMOMECHANICAL LOADING CONDITIONS

Loading conditions used in the notched-panel analyses were derived from SST flight conditions presented in Reference 2. Typical flights, taken from Reference 2, are shown in Figure 3.2-1 which identifies the two stress sequences considered in this study. The Type-A stress sequence accounts for the stresses caused by gusts, maneuvers and ground-air-ground (GAG) cycles. The Type-C stress sequence accounts for effects of temperature gradients within the SST wing structure in addition to the Type-A stresses. A summary of the four problems consisting of the twelve flights which were analyzed is presented in Table 3.2-I. The nomenclature is consistent with Reference 2.

Two of the simulated flights from Reference 2 were selected for analysis as representative stress sequences for the SST lower wing surface under operational conditions. In problem I, the local stresses and strains were calculated for 3 repetitions of a Type-A flight. The simplified load-temperature profile is shown in Figure 3.2-2.

In problem II, stresses and strains were calculated for 5 consecutive Type-C flights, (see Table 3.2-I and Figures 3.2-3 and 3.2-4); the first two flights contain loads expected to occur in every operational flight, the next two flights (flight numbers 6 and 7) contain loads expected to occur during every thousandth operational flight, and the last flight in problem II is the same as the first two flights of this set. Thus, the calculations were expected to show the effects of an infrequent severe flight on the local stresses and strains at a typical notch.

In problems III and IV, Type-C flights were analyzed with different values of the design mean stress so the relative magnitudes of local stresses and strains could be assessed for a range of design stresses. The simplified flights for these problems are shown in Figure 3.2-3.

3.2 (Continued)

The applied stresses and temperatures used in the simplified flight model of each of the problems are shown in Figures 3.2-5, 3.2-6 and 3.2-7.

The most significant difference between the various flight models is the loading condition prior to the increase in temperature. Flights 1, 2, 3, 6 and 7 progress from zero load to maximum loading, Point A, that occurs during climb, followed by a reduction in applied load to point B. Loading is then held constant while temperature is increased between points B and C. Flights 4, 5, and 8 through 12 progress from zero load to a maximum loading at point A with loading held constant while temperature is increased between points A and B. For the purpose of discussion of the analytical results, Flights 1, 2, 3, 6 and 7 are designated as Flight Configuration I. Flights 4, 5, and 8 through 12 are designated as Flight Configuration II.

All flights include a ninety-minute period of constant load and temperature to simulate supersonic cruise. During the simulated cruise creep at the notch was evaluated. These creep conditions are defined by two 45-minute periods of constant applied stress and temperature. Midway through the cruise period, a single stress excursion is applied for all flights. The excursion represents a typical stress that occurs during cruise.

At the end of each cruise period temperature is reduced to the initial temperature and then loading is reduced to represent the minimum net stress in the GAG cycle. The cycle is closed by increasing the minimum net stress back to zero.

THIS PAGE LEFT INTENTIONALLY BLANK.

4.0 FINITE-ELEMENT MODEL

Since the panel was subjected to a uniform temperature distribution at all times and the panel and its loading conditions were symmetrical, it was possible to analyze only one quadrant of the panel. The selected quadrant and the boundary conditions imposed on the model are shown in Figure 4.0-1. These boundary conditions permit free expansion/contraction with change in temperature, and maintain compatibility along the inner boundaries of the model.

The BOPACE program [4] provides the constant-strain-triangle (CST) for thermal, elastic, plastic, and creep analysis. Options are provided for plane-stress, plane-strain, or limited 3-dimensional analysis involving prescribed non-zero values of normal stress or strain; the appropriate model for the notched panel problem is the plane-stress CST.

Based on previous experience with the BOPACE program it was estimated that a model consisting of approximately 200 nodes (400 degrees of freedom) would be sufficient to accurately determine distributions of stress and strain within the panel. To verify the accuracy of the model, three models were developed and tested.

The first model consisted of a relatively coarse mesh and was used to obtain estimates of the elastic stress concentration at the notch. The first model consisted of 114 nodes and 192 plane-stress elements. The stress concentration obtained with the coarse mesh was 3.87. The experimentally determined value of the stress concentration factor at the notch is 4.1.

The second model was generated from the coarse mesh by dividing each of the elements into four elements. The second model, consisting of 437 nodes and 768 elements, was used to assess convergence to the true stress concentration. The stress concentration obtained with the second model was 3.94.

4.0 (Continued)

Since the major portion of the panel was expected to remain elastic under the flight conditions prescribed in Section 3.2 it was decided to maintain a fine mesh only in the area of the notch. The third model, generated from model number 2 consisted of further refinements near the notch and a relatively coarse mesh over the remaining portion of the model. The third model consisted of 141 nodes and 222 elements and is shown in Figure 4.0-2. The size of elements surrounding the notch in model three ranged from 0.032 sq.mm. on the X-axis and 9.54 sq.mm. on the Y-axis. The areas of all elements in the region of maximum stress concentration (elements 201 through 206) are less than 0.1 sq.mm. The stress concentration obtained with the third model was 4.00.

A comparison of the elastic stress distributions along the X-axis of models two and three is shown in Figure 4.0-3. Model number three was selected for analysis of the prescribed flight conditions.

4.1 ELASTIC-PLASTIC STRESS-STRAIN BEHAVIOR AT CONSTANT TEMPERATURE

The stress-strain curves of Figure 3.1-2 were idealized for use in the BOPACE analysis. Material properties are input as tabular values in BOPACE and a linear variation between input data points is assumed. The assumed piecewise linear stress-strain plots are shown in Figure 4.1-1. The apparent deviation from linearity in the uniaxial stress-strain diagrams was defined as the yield point. It is believed that this definition of yield provides a more accurate representation of the material than a yield point defined by the 0.2 percent strain offset method. The definition of yield in BOPACE is not arbitrary because every definition of yield gives rise to a different yield surface and for a complex but specific loading history each definition gives rise to a different plastic strain history.

4.1 (Continued)

Since the mechanical properties of Figure 3.1-2 characterize cyclic-strain-stabilized material, the hardening was assumed to be only kinematic. This means that the size of a stress-strain hysteresis loop for the Ti-6Al-4V did not change for repetitions of a given flight loading. The kinematic hardening, however, resulted in a slight translation of the hysteresis loops and a significant Bauschinger effect. In order to perform the analysis of the notched panel it was necessary to define kinematic hardening behavior when changing the panel temperature. The hardening effects of variable temperature are illustrated in Figure 4.1-1. As long as the temperature is constant plastic hardening is defined by following the shape of the stress-strain curve at the given temperature, say to point 0 on the 297°K curve. If the temperature changes and plastic deformation continues, an initial point must be established from which the new yield surface size and hardening slope may be determined. The transfer from the low to high temperature condition requires a definition of the type of hardening exhibited by the material. BOPACE provides the option of either plastic work or the sum of increments of effective plastic strain to be used as the hardening basis. The work and strain options correspond to the respective points 1 and 2 in Figure 4.1-1. Strain hardening behavior was assumed for Ti-6Al-4V titanium, but the choice between plastic work and plastic strain as a basis for hardening depends on which basis best represents behavior and should be verified by test. Details concerning the hardening theory and its implementation in BOPACE are presented in Reference 4.

4.2 CREEP BEHAVIOR

Metals characteristically exhibit primary, secondary and tertiary creep. The creep data in Figures 3.1-4 and 3.1-5 reflect the first two stages, but the initial portion of primary creep is not well defined. For this reason certain assumptions had to be made regarding primary creep behavior.

4.2 (Continued)

The BOPACE approach to creep analysis requires that a reference creep curve shape be defined for each material to be analyzed. The reference creep curve defines the relative variation of effective-creep-strain as a function of time. This shape is assumed valid for all temperatures and stress levels of a given material. The reference curve for this study was the room temperature (297.0°K) creep curve at a constant stress level of 930.8 N/mm^2 (Figure 3.1-4). This curve provided the best definition of the initial portion of primary creep but still required an assumption regarding the amount of strain shown at zero-time. The curve of Figure 3.1-4 indicates 0.6 percent strain at zero time. Thus the 0.6 percent value was considered to be a time-independent strain and creep was assumed to commence from that point; i.e., the BOPACE reference creep curve is the 930.8 N/mm^2, 297.0°K curve of Figure 3.1-4 shifted down by 0.6 percent strain. The reference creep curve used is shown in Figure 4.2-1.

Creep data for the material at temperatures and stresses different from the reference curve are determined by multiplying the reference curve by appropriate factors to approximate Ti-6Al-4V creep behavior as a function of temperature and effective stress. Only data at 560.9°K are required for the creep analysis because the simulated flights of Section 3.2 consider the occurrence of creep only at the elevated temperature.

Figure 3.1-5 indicates that measurable creep rates at the elevated temperature are independent of stress at levels equal to or greater than 620 N/mm^2. It was again assumed that the values of strain for the elevated temperature curves at zero-time correspond to elastic-plastic (time-independent) behavior. This means a single shape describes creep behavior at the elevated temperature for effective stresses greater than 620 N/mm^2. A single multiplication factor of 0.061 was applied to the reference curve for definition of elevated

4.2 (Continued)

temperature creep at stresses above 620 N/mm^2. The factor was determined from the ratio of creep strain for the two temperatures at time equal to 90 minutes.

The threshold stress for onset of creep in an initially unstrained material at elevated temperature is indicated by the 620 N/mm^2 curve of Figure 3.1-5. This value was used to determine creep initiation during preliminary assessment of notched panel behavior, but the relatively large difference in creep between stresses of 620 and 655 N/mm^2 at elevated temperature caused numerical stability and convergence problems in the BOPACE analysis. It was necessary to smooth out this approximate jump condition and this was accomplished by reducing the threshold stress to 500 N/mm^2. The solution was stable and convergence rapid when using the lower threshold stress. Accurate definition of threshold stress is desirable because residual effects at the notch in unloaded panels are dependent upon creep deformations.

The hardening that occurs during creep is determined by following the creep curve as long as temperature and stress remain constant. For the present analysis, the applied load and temperature are constant for all simulated cruise conditions, but the local effective stresses change as creep occurs. When the local stress is between the threshold value and 655 N/mm^2 an initial point for the given time increment must be defined on the corresponding new creep curve to determine the new creep rate. The transfer from one curve to another requires an assumption for creep hardening. BOPACE provides options of age, strain, or work hardening. Details concerning these hardening assumptions are found in References 4 and 5. The strain hardening option was used to define creep hardening behavior of the Ti-6Al-4V material; strain hardening is generally assumed and was used in this study because data were unavailable to determine which hardening assumption best characterizes creep in titanium.

4.3 SUMMARY OF ASSUMPTIONS CONCERNING BEHAVIOR OF Ti-6Al-4V TITANIUM

The development of the notched panel model consisted of several critical assumptions necessary to characterize the Ti-6Al-4V titanium. These assumptions were:

1. The material is isotropic in stress and strain.

2. The yield point is defined as the deviation from linearity in the uniaxial stress-strain curve at temperature.

3. The material was cyclically stabilized with the result that no isotropic hardening will occur under the specified SST conditions.

4. The temperature effect on Bauschinger kinematic hardening is a function of effective plastic strain.

5. The temperature effect on creep hardening is a function of effective creep strain.

6. Material strain hardening behavior is affected by temperature variations only in an incremental sense; cumulative strain hardening is unaltered by change in temperature.

These assumptions may significantly affect the analytical results and should be further investigated by testing of simple uniaxial specimens. Should certain of the assumptions prove to be inadequate, modifications of the model should be incorporated and subsequent BOPACE analyses performed to better predict behavior of the titanium panel.

Since the greatest portion of the hysteresis loops shown in Section 5 is determined by plastic deformations under variable load and temperature, plastic flow is probably the most damaging mechanism in Ti-6Al-4V titanium for the specified load-temperature conditions. For this reason,

4.3 (Continued)

the assumptions concerning plastic behavior should receive particular attention. For example, some unpublished experimental data indicate that Ti-6Al-4V titanium has no memory of previous strain history if heated to 560°K and strained plastically subsequent to plastic straining at 297°K. Thus, assumption number 6 may not be entirely reconcilable with actual Ti-6Al-4V behavior. Consequently, this assumption, as well as the others, should be investigated before the results can be used in a quantitative damage assessment of the notched panel.

THIS PAGE LEFT INTENTIONALLY BLANK.

5.0 ANALYTICAL RESULTS

The finite-element analyses of flight conditions defined in Section 3.2 provide structural behavior of the entire panel. Attention was focused however upon response in the region of the notch. It is in this region that the most damaging behavior consisting of plastic and creep deformations occur.

The inelastic behavior of material at the notch is characterized by stress-strain hysteresis loops for element 201 (see Figure 4.0.2). Variations in stress in regions removed from the notch are also presented for various flight conditions.

5.1 FLIGHT CONFIGURATION I RESULTS

Behavior of the notched panel under the variable load-temperature conditions of Configuration I flights is characterized by the stress-strain hysteresis loops of Figure 5.1-1 and 5.1-2. The significant load-temperature points of Figure 3.2-1 are identified on the loops. Intermediate points are shown where changes in slope occurred for a given load, temperature or time increment. The load increments used in the analysis did not clearly define the yield point under reversed loading, but it was possible to estimate this value by using the following procedure which was typical for all flights. In Figure 5.1-1, the stress-strain curve was extended from point G along a line parallel to the linear portion of the left-hand side of the loop. Since there was no isotropic hardening, the range of stress from point A to the yield point in compression was the same as the range from point H to the yield point in tension. Thus, the compressive yield point could be estimated and is shown as the break point with no symbol. Since the relative magnitudes of stress-strain components other than longitudinal (y-directed) values were negligibly small at the notch, only the longitudinal components are plotted.

5.1 (Continued)

Conditions at the notch for flights 1, 2 and 3 are shown in Figure 5.1-1. This figure clearly shows the result of the assumption of zero isotropic hardening in the cyclic stabilized material; there is no change in the size of the hysteresis loop from cycle-to-cycle.

A pronounced Bauschinger effect resulted from the assumed kinematic hardening but this effect completely stabilized after the second cycle. The Bauschinger kinematic hardening effect is apparent in that initial yielding in tension caused a reduced yield in compression. The successive yielding in compression was not large enough to significantly change the yield stress in tension during the second cycle (flight 2).

No horizontal translation of the loops occurred because neither creep nor plastic flow occurred under flights 1, 2 and 3 elevated temperature conditions. Also, the inelastic work which occurred during the first three flights was unaffected by sustained loading at elevated temperature.

An interesting phenomenon did result from the temperature changes in the Configuration I flights. Unloading from point A carried the model well into the elastic range at point B. The loading was held constant while the temperature was incrementally increased uniformly throughout the model. Even though the temperature change amounted to 250°C, the local strains and stresses remained in the elastic range. Consequently the temperature increase which caused an approximate 15 percent decrease in model stiffness resulted in increased nonuniform elastic deformations throughout the model. If the change in elastic strains had been uniform (as in an unnotched specimen), no net change in stresses would have occurred under constant load and increased temperature. The notch, however, causes a nonuniform increase in elastic strain with temperature. In fact the change in stress at the notch was larger than the average net effect by the elastic concentration

5.1 (Continued)

factor of 4. To fix ideas concerning this behavior it is necessary to review the theory behind the elastic stress calculations in BOPACE. Changes in stress are computed from a simple algorithm based on the functional relation between elastic stress and strain $\sigma = E\ \varepsilon$; E is the elastic modulus and σ and ε are uniaxial stress and strain. An increment in stress is $d\sigma = dE \cdot \varepsilon + E\ d\varepsilon$ or in an average sense $\Delta\sigma = \Delta E \cdot \varepsilon_0 + E_1 \cdot \Delta\varepsilon$ where subscripts 0 and 1 denote initial and final conditions respectively for a given increment. The operation is illustrated in Figure 5.1-3 wherein the model, initially at uniform temperature T_0, undergoes a uniform temperature change to T_1. The local strains at T_1 are determined from the incremental force-elastic stiffness relations and the increment in local stress is calculated from the equations above.

The stress-strain behavior for loading conditions B to G in flights 1, 2, and 3 was entirely elastic. Consequently any fatigue damage caused by the cruise condition in the first three flights would be associated with high-cycle fatigue. The inelastic behavior reflected in the hysteresis loops would have a significant effect upon the low-cycle fatigue life. No attempt was made during this study to assess fatigue damage in the notched panel, but the approach presented here would be useful in a damage assessment based upon techniques such as the strain-range partitioning approach of Halford, Hirschberg and Manson [6, 7].

Figure 5.1-2 shows the hysteretic behavior at the notch for flights 6 and 7 which were started from the residual effects at the end of flight 5. The significant difference between these loops and those of Figure 5.1-1 is in the response to elevated temperature and loading from C to D. The behavior for flights 6 and 7 was elastic-plastic at the notch between these points. The plastic response between C' and D resulted in a horizontal translation of the loops because no inelastic

5.1 (Continued)

reversal of strain occurred at elevated temperature. Thus a decreasing racheting effect was observed in these two flights. As previously stated in Section 3.2, flights 6 and 7 were analyzed to study the effects of an infrequent severe flight on local stresses and strains at the notch. These effects on flight 8 are discussed in Section 5.2.

5.2 FLIGHT CONFIGURATION II RESULTS

Behavior of the notched panel under Configuration II flight conditions is shown in Figures 5.2-1 through 5.2-7. The hysteresis loop for Configuration I flight is also replotted in Figure 5.2-2 to show comparative behavior and interaction between flights 5, 7 and 8. The significant differences in structural response to the two different flight configurations occur during the temperature rise and initial 45-minute creep periods. No inelastic behavior occurred during these periods in flights 6 and 7 whereas both plastic and viscoelastic deformations were existent at the notch for all Configuration II flights.

Material at the notch was plastically deformed at point A and temperature was increased with no reduction in load for Configuration II flights. Consequently plastic flow continued with incremental temperature increases and the stress decreased monotonically with strain. Since stress at the end of the temperature increase was above the threshold value, creep occurred during the 45-minute period of constant temperature and applied load.

A more detailed representation of the temperature effects under constant loading for flights 4, 5 and 8 is shown in Figure 5.2-3. The results in this figure are typical of the notch behavior in all Configuration II flights. Creep behavior is exhibited by the successive reduction in creep. The strains were viscoelastic between points BB'; i.e., no plastic flow occurred in this period. This was to be expected since the

5.2 (Continued)

material at the notch was unloading under constant temperature and applied load, and local effective stresses were below the current yield point established by prior plastic straining and the current temperature. Current values of yield or creep threshold stresses are computed by BOPACE in accordance with assumed hardening behavior and are used by the program to calculate inelastic behavior for a current load-temperature increment. Increased loading after the initial creep periods resulted in elastic-plastic deformations to point C. This was followed by a reduction in applied load to the value at point D which gave notch stresses below the threshold value for creep. Thus no additional creep occurred during the second 45-minute creep period in any given flight. The temperature decrease at constant load from point D' to E resulted in elastic unstraining like that exhibited in Configuration I flights. The significant difference in horizontal translation between flights 4, 5 and 5, 8 (see Figure 5.2.3) resulted from the cumulative plastic strain which occurred at elevated temperature during flights 6 and 7.

Figures 5.2-4 and 5.2-5 show notch stress-strain behavior for flights 9, 10 and 11, 12 respectively. The applied loads for these two sets of flights were respectively 84 percent and 116 percent of the loading for flights 4, 5 and 8. The difference in maximum notch stress varied less than 10 percent between the three sets of flights because of the relatively small change in stress with strain for strains greater than 0.8 percent in titanium.

Figure 5.2-6 shows the variation in stress in the vicinity of the notch for flight 4. This plot is typical of results obtained for all flights. The left-hand portion of curves E and G in Figure 5.2-6 where the slopes change respectively from positive-to-zero and negative-to-zero, indicate the plastic zone along the X-axis. Figure 5.2-7 shows details in stress variations in the immediate area of the notch for flight 4. The curves of Figure 5.2-8 result from the

5.2 (Continued)

cumulative strain-temperature history but reflect the stress-strain condition for the current load, time or temperature increment. For example, curve E indicates that the stress-strain behavior at point E is elastic at y = 0. Previous behavior which resulted in permanent effects are existent at E in the form of creep and plastic deformations, but unstraining caused by temperature reduction has carried the structure to a totally elastic state. Thus, strains in the material near the notch consisted of elastic-plastic behavior for increments OA, AB, and BC, viscoelastic behavior at point B', and completely elastic behavior at points D, D' and E. In general, the panel was elastic for the entire flight in the interval $40 < X \leq 151.13$ mm at y = 0. The zone of inelastic deformation was highly localized.

6.0 CONCLUDING REMARKS

The objective of this study was to demonstrate the feasibility of using the finite-element method to account for the effects of cyclic load and temperature on local stresses and strains at a notch. The results show the approach is feasible and provides an efficient method for obtaining solutions necessary in the evaluation of fatigue damage of an SST structure. The results indicated were computed by using approximately 30 load/temperature increments for each flight; rather rapid convergence was observed at each increment and the average run time per flight was 30-minutes on an IBM 370/155 computer.

Before the results can be applied with confidence it will be necessary to gain improved understanding of material response to cyclic loads, temperatures and hold times. The constitutive assumptions which may significantly affect the hysteretic behavior at the notch were discussed in some detail in Section 4. These assumptions should receive particular attention in any subsequent effort related to this study.

REFERENCES

1. Imig, L. A.; and Garrett, L. E.: Fatigue-Test Acceleration with Flight-by-Flight Loading and Heating to Simulate Supersonic Transport Operation. NASA TN D-7380, December 1973.

2. Imig, L. A.: Fatigue of SST Materials Using Simulated Flight-by-Flight Loading. Presented at the ASTM/ASME/ASM/U. Conn. Symposium on Fatigue at Elevated Temperatures, Storrs, Connecticut, June 1972.

3. Imig, L. A.; and Illg, Walter: Fatigue of Notched Ti-8Al-1Mo-1V Titanium Alloy at Room Temperature and 550°F (560°K) with Flight-by-Flight Loading Representative of a Supersonic Transport. NASA TN D-5294, July 1969.

4. BOPACE Theory and User Documentation; Boeing Document D5-17266-1 and -2; NAS8-29821 (1-3-50-32679 [1F]); George C. Marshall Space Flight Center, Alabama; 1973.

5. Manson, S. S.; Thermal Stress and Low-Cycle Fatigue; McGraw-Hill Book Co.; 1966.

6. Manson, S. S. Halford, G. F. and Hirschberg, M. H.: Creep-Fatigue Analysis by Strain-Range Partitioning; Symposium on Design for Elevated Temperature Environment, Am. Soc. Mech. Eng.; 1971.

7. Halford, G. R., Hirschberg, M. H. and Manson S. S.; Temperature Effects on the Strainrange Partitioning Approach for Creep-Fatigue Analysis; NASA TMX-68023; 1972.

DEFINITION OF ELLIPSE:

$$\frac{X^2}{955.486} + \frac{Y^2}{281.936} = 1$$

MATERIAL:

TITANIUM ALLOY Ti-6Al-4V

DUPLEX ANNEALED

1.35 mm THICK SHEET

STRESS CONCENTRATION FACTOR:

K(experimental) = 4.1

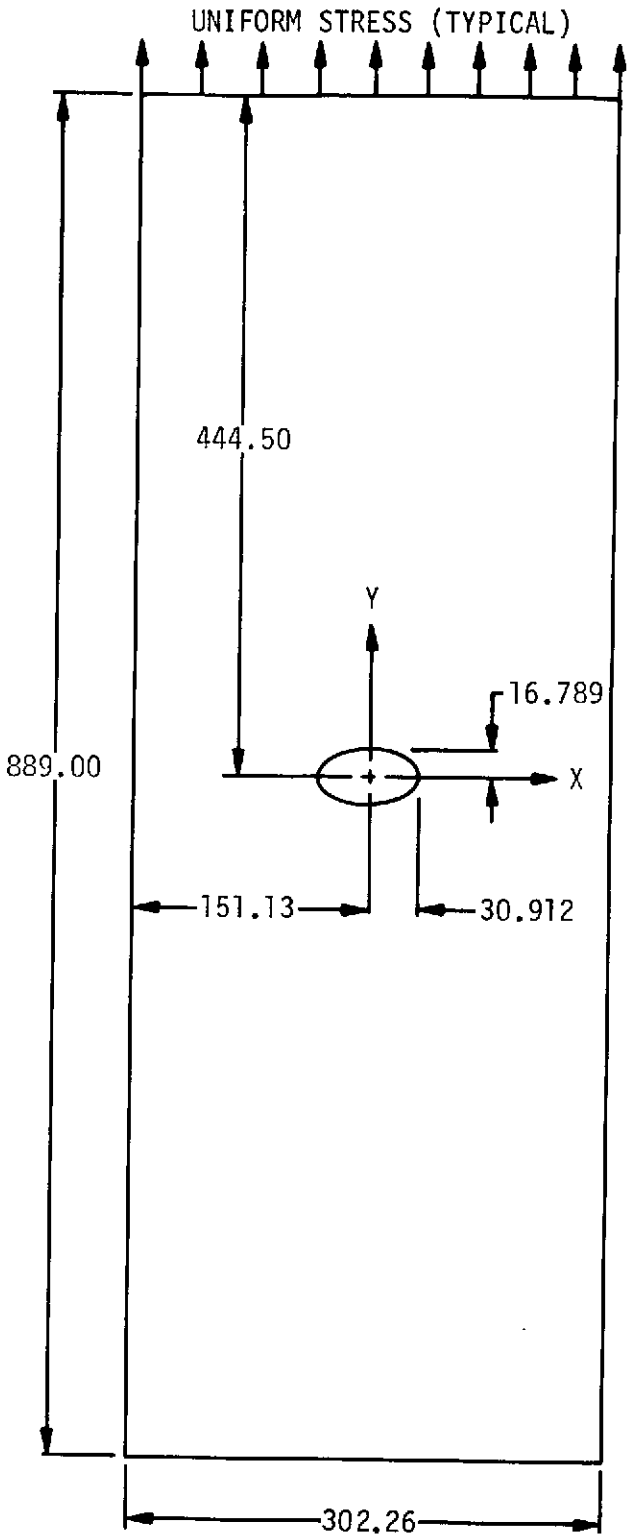

FIGURE 3.1-1: NOTCHED PANEL CONFIGURATION
DIMENSIONS IN MILLIMETERS

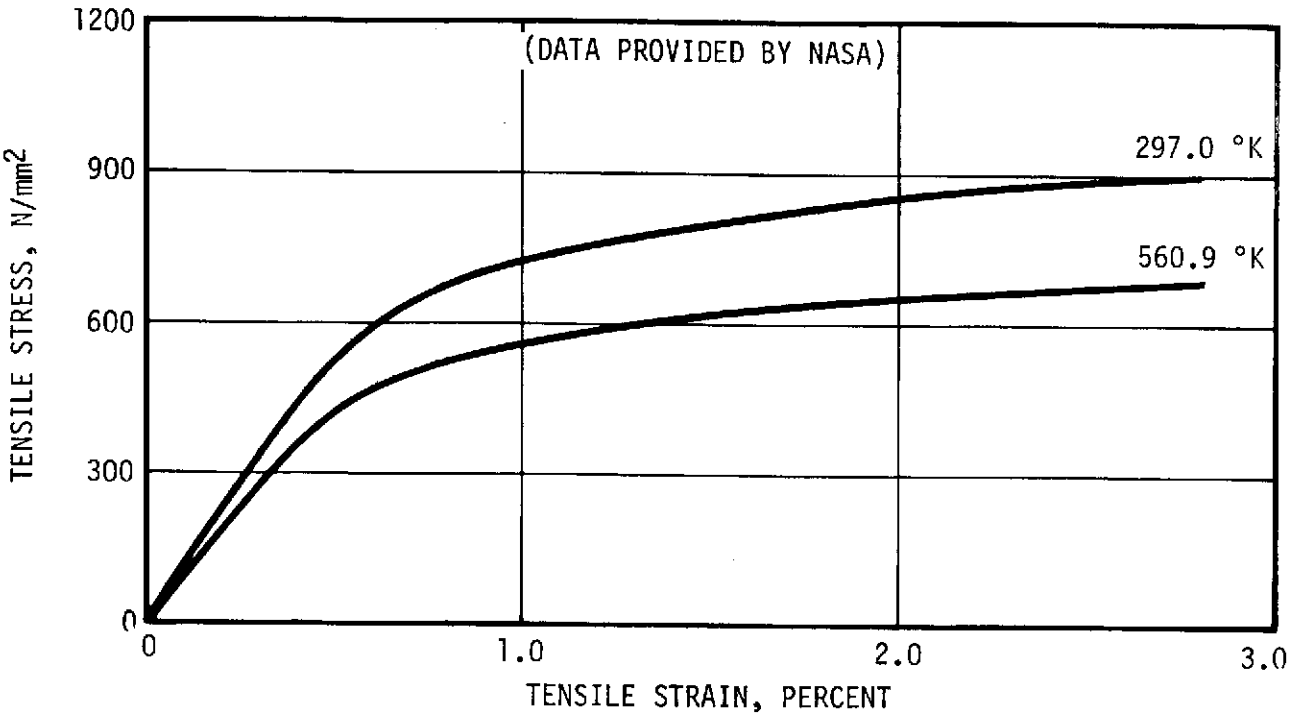

FIGURE 3.1-2: TENSILE STRESS-STRAIN CURVES FOR CYCLICALLY-STRAIN-STABILIZED Ti-6Al-4V DUPLEX ANNEALED TITANIUM ALLOY (BAR)

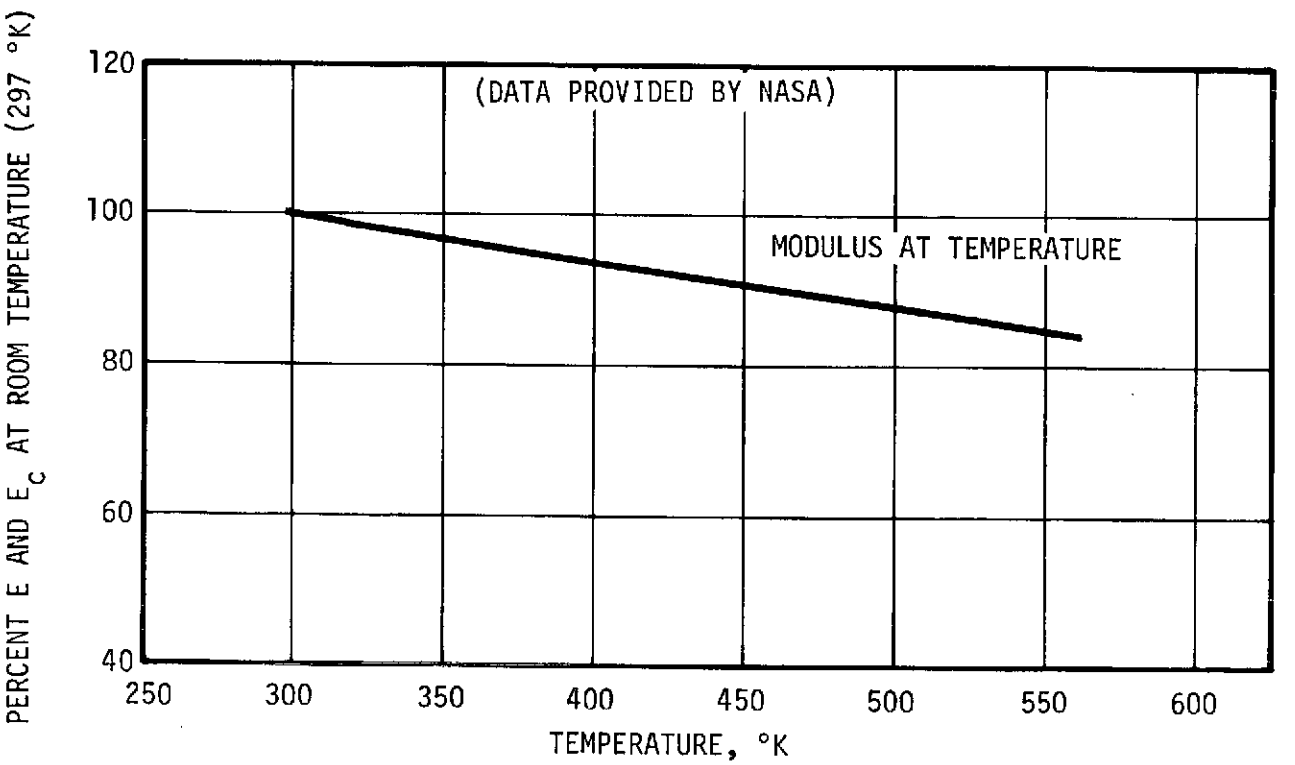

FIGURE 3.1-3: EFFECT OF TEMPERATURE ON TENSILE AND COMPRESSIVE MODULUS (E AND E_c) OF Ti-6Al-4V TITANIUM ALLOY

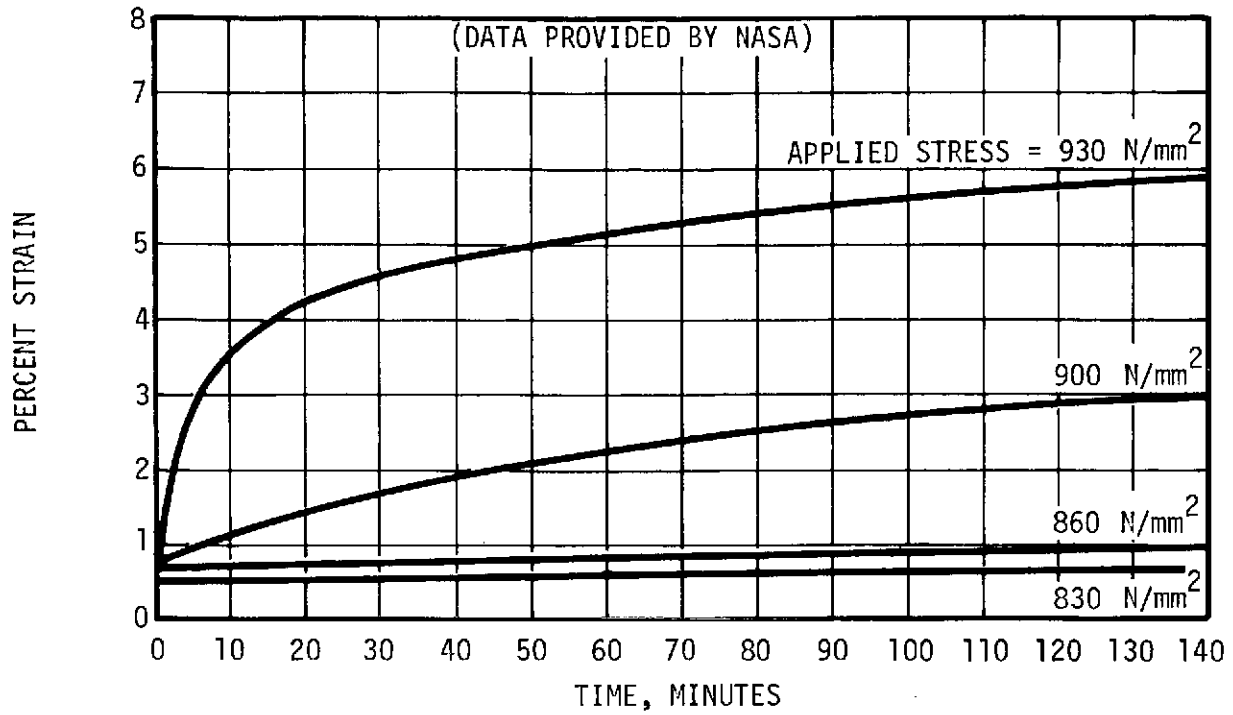

FIGURE 3.1-4: CREEP CURVES FOR Ti-6Al-4V DUPLEX ANNEALED TITANIUM ALLOY (SHEET) AT 297.0 °K

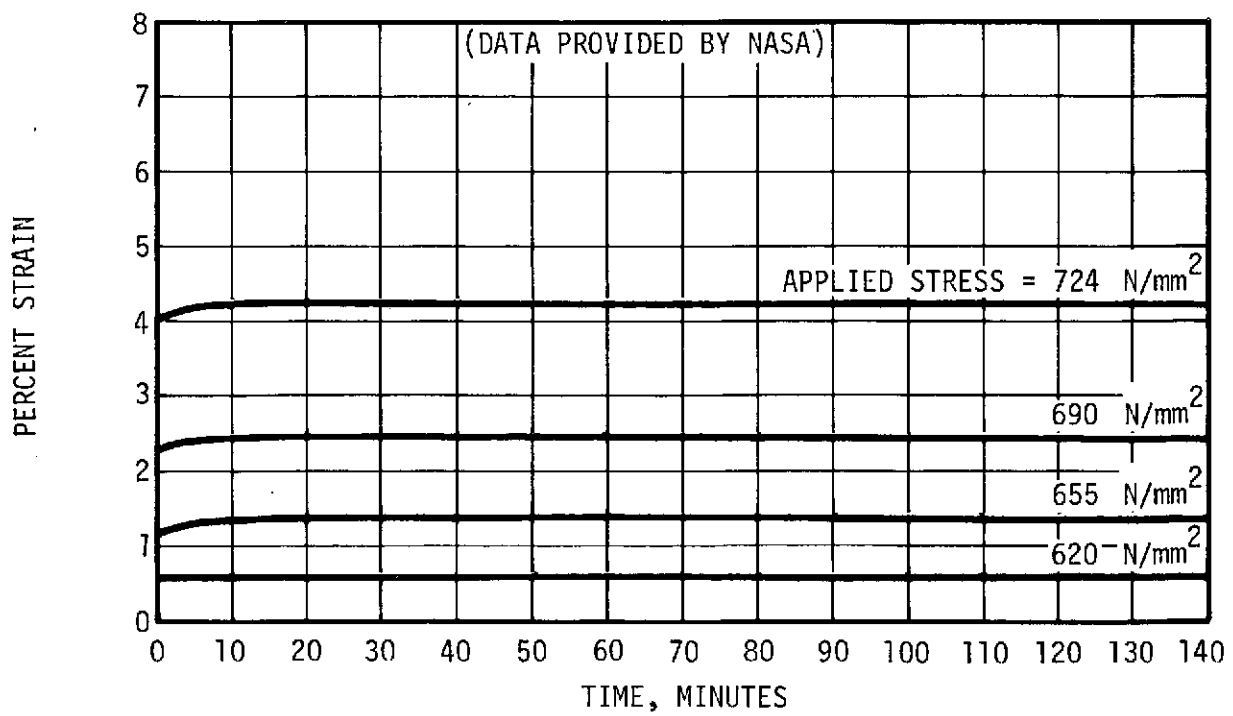

FIGURE 3.1-5: CREEP CURVES FOR Ti-6Al-4V DUPLEX ANNEALED TITANIUM ALLOY (SHEET) AT 560.9 °K.

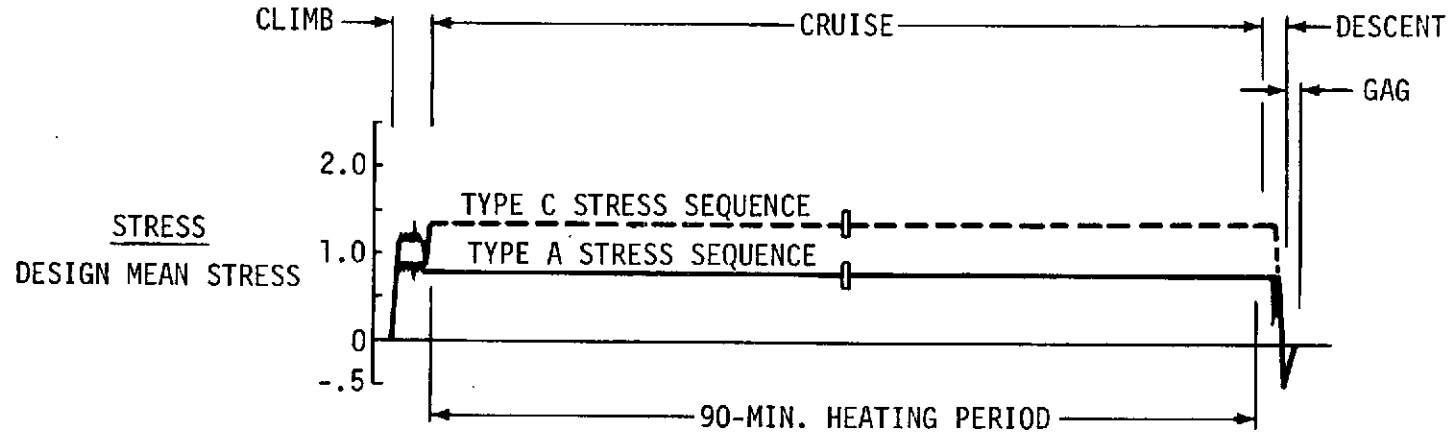

FIGURE 3.2-1: STRESS SEQUENCES FOR SIMULATED FLIGHTS FROM REFERENCE 2

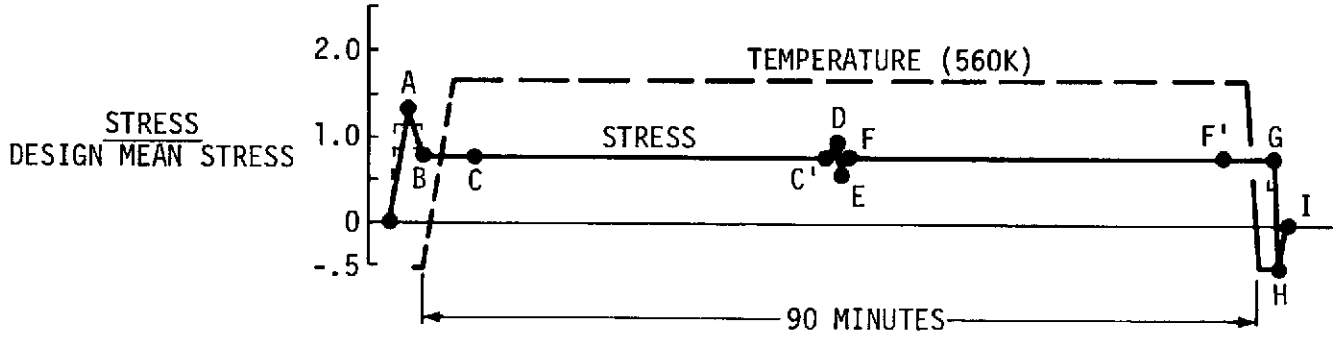

FIGURE 3.2-2: SIMPLIFICATION OF TYPE-A STRESS SEQUENCE USED IN FINITE-ELEMENT ANALYSIS FOR FLIGHTS 1, 2 AND 3

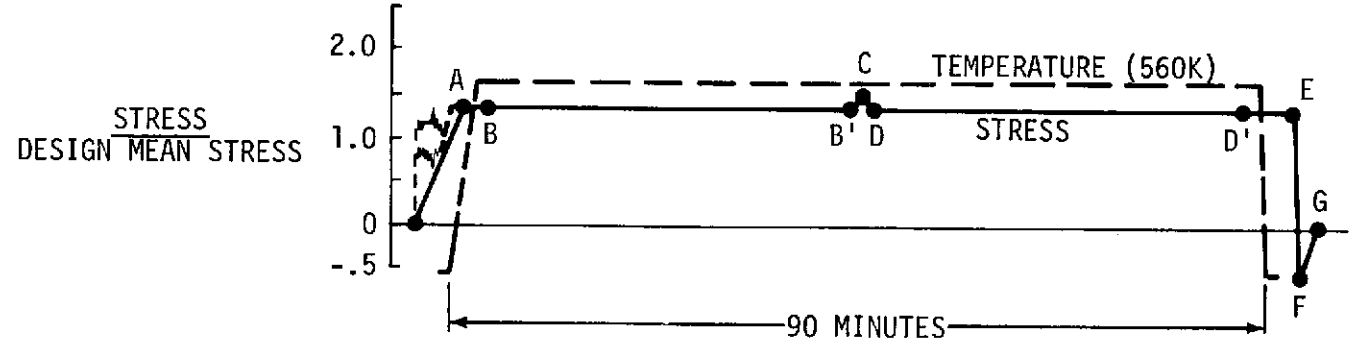

FIGURE 3.2-3: SIMPLIFICATION OF TYPE-C STRESS SEQUENCE USED IN FINITE-ELEMENT ANALYSIS FOR FLIGHTS 4, 5, AND 8-12

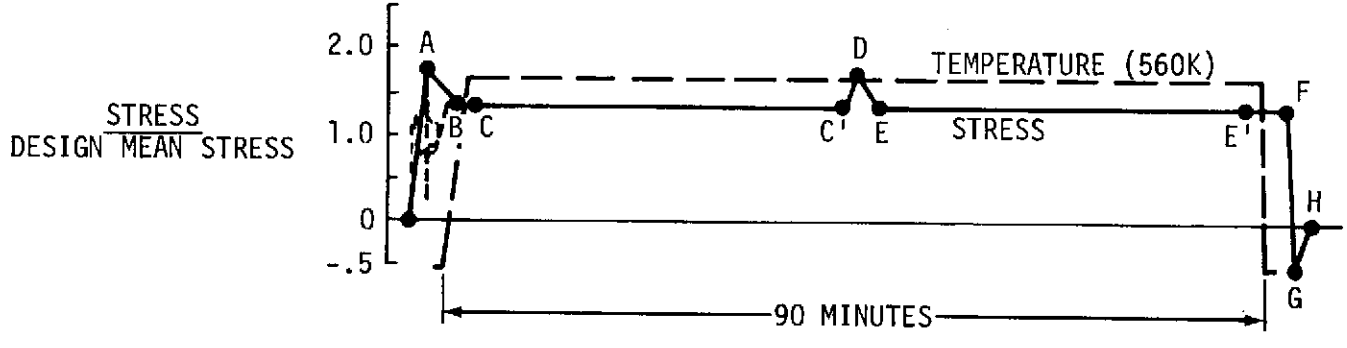

FIGURE 3.2-4: SIMPLIFICATION OF TYPE-C STRESS SEQUENCE USED IN FINITE-ELEMENT ANALYSIS FOR FLIGHTS 6 AND 7

LOAD-TEMPERATURE PROFILE

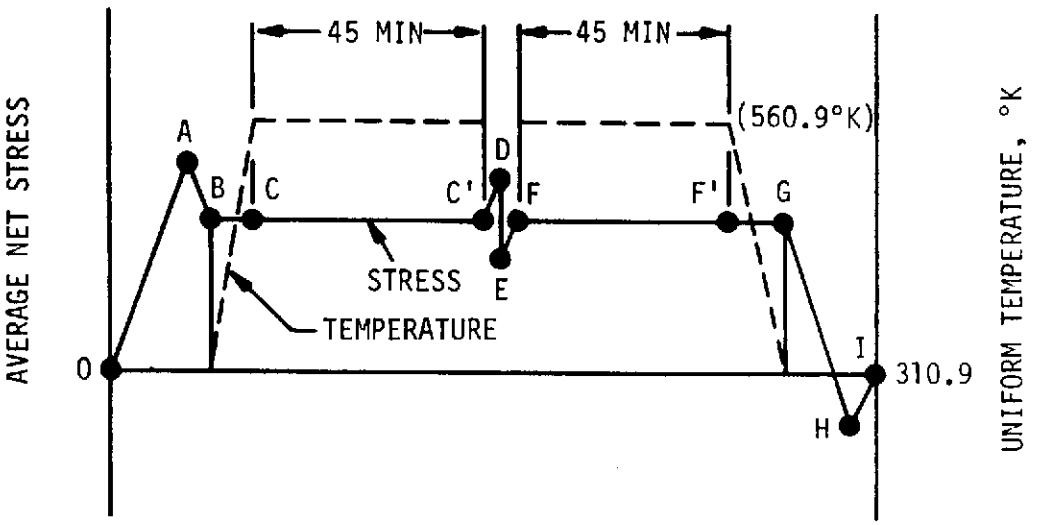

APPLIED STRESS

POINT	AVERAGE NET STRESS (N/mm^2)
	FLIGHT 1, 2, 3
A	348
B	195
C	195
C'	195
D	231
E	158
F	195
F'	195
G	195
H	-130
I	0

NOTES:
1. CREEP ANALYSIS PERFORMED FOR 45-MINUTE PERIODS OF CONSTANT STRESS AND TEMPERATURE.
2. FLIGHT 1 BEGINS WITH PANEL IN INITIAL (UNSTRAINED) CONFIGURATION.
3. BEGIN FLIGHT 2 WITH POINT I1.
4. BEGIN FLIGHT 3 WITH POINT I2.

FIGURE 3.2-5: SIMPLIFIED MODEL OF LOADS AND TEMPERATURES USED IN ANALYSIS OF FLIGHTS 1, 2, AND 3. (FLIGHT CONFIGURATION I)

LOAD-TEMPERATURE PROFILE

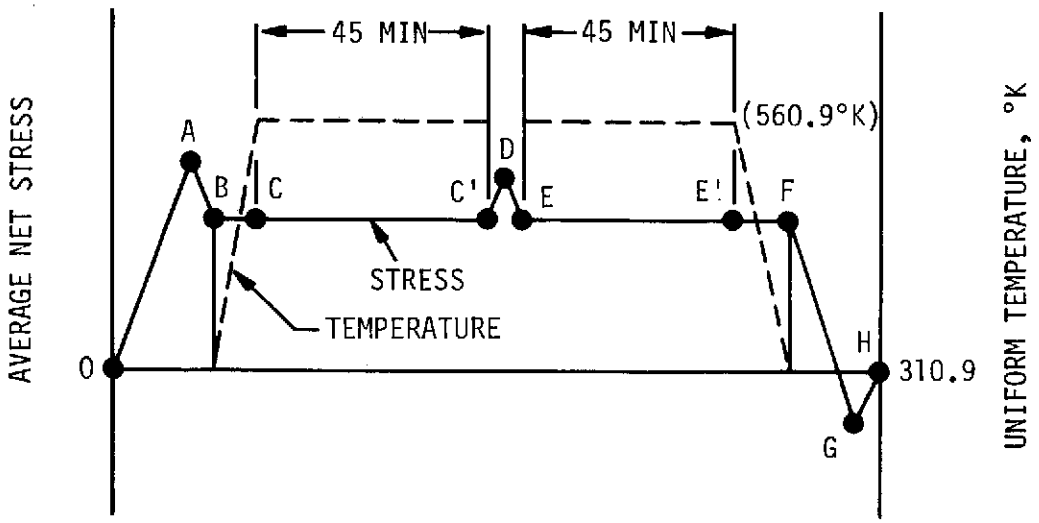

APPLIED STRESS

POINT	AVERAGE NET STRESS (N/mm^2)
	FLIGHT 6, 7
A	381
B	279
C	279
C'	279
D	370
E	279
E'	279
F	279
G	-103
H	0

NOTES:
1. CREEP ANALYSIS PERFORMED FOR 45-MINUTE PERIODS OF CONSTANT STRESS AND TEMPERATURE.
2. BEGIN FLIGHT 6 WITH POINT G5 OF CONFIGURATION II.
3. BEGIN FLIGHT 7 WITH POINT H6.

FIGURE 3.2-6: SIMPLIFIED MODEL OF LOADS AND TEMPERATURES USED IN ANALYSIS OF FLIGHTS 6 AND 7. (FLIGHT CONFIGURATION I)

LOAD - TEMPERATURE PROFILE

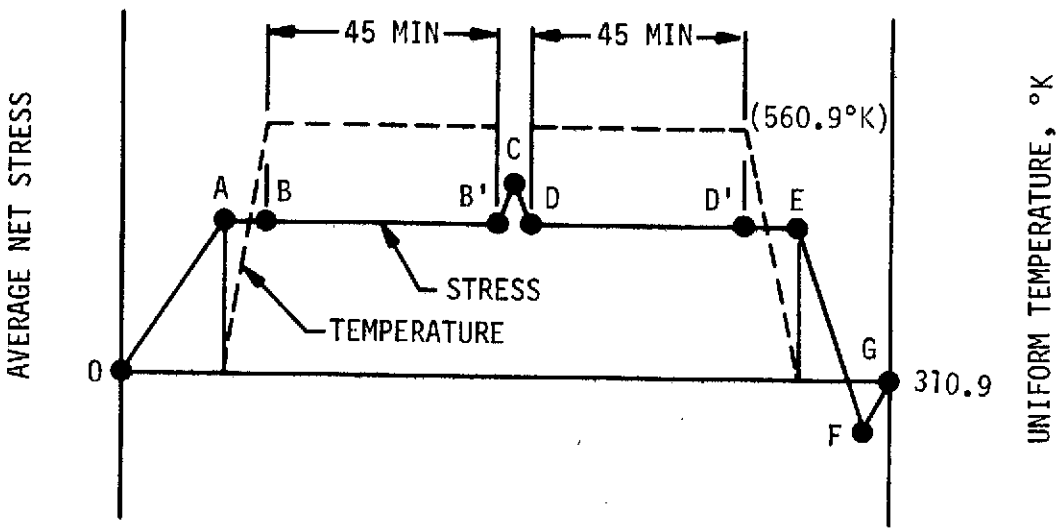

APPLIED STRESS

POINT	AVERAGE NET STRESS (N/mm^2)		
	FLIGHT 4, 5, 8	FLIGHT 9, 10	FLIGHT 11, 12
A	279	233	325
B	279	233	325
B'	279	233	325
C	308	256	360
D	279	233	325
D'	279	233	325
E	279	233	325
F	-103	- 86	-121
G	0	0	0

NOTES:
1. CREEP ANALYSIS PERFORMED FOR 45-MINUTE PERIODS OF CONSTANT STRESS AND TEMPERATURE.
2. FLIGHT 4, 9, 11 BEGIN WITH PANEL IN INITIAL (UNSTRAINED) CONFIGURATION.
3. BEGIN FLIGHT 5 WITH POINT G4.
4. BEGIN FLIGHT 8 WITH POINT H7 OF CONFIGURATION I.
5. BEGIN FLIGHT 10 WITH POINT G9.
6. BEGIN FLIGHT 12 WITH POINT G10.

FIGURE 3.2-7: SIMPLIFIED MODEL OF LOADS AND TEMPERATURES USED IN ANALYSIS OF FLIGHTS 4, 5 AND 8-12.

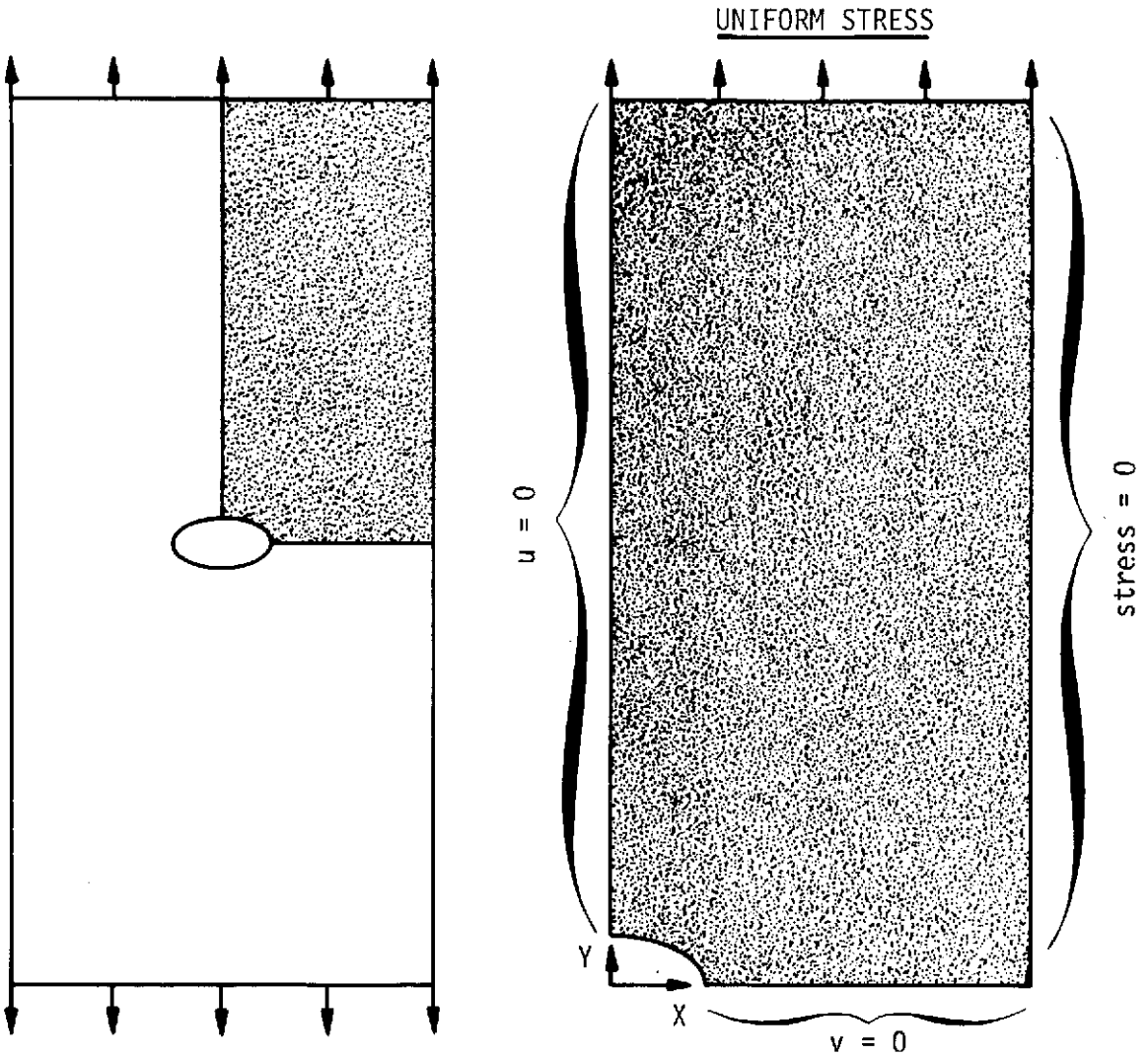

u = DISPLACEMENTS IN X-DIRECTION

v = DISPLACEMENTS IN Y-DIRECTION

FIGURE 4.0-1: SECTION OF PANEL SELECTED FOR ANALYSIS AND IMPOSED BOUNDARY CONDITIONS

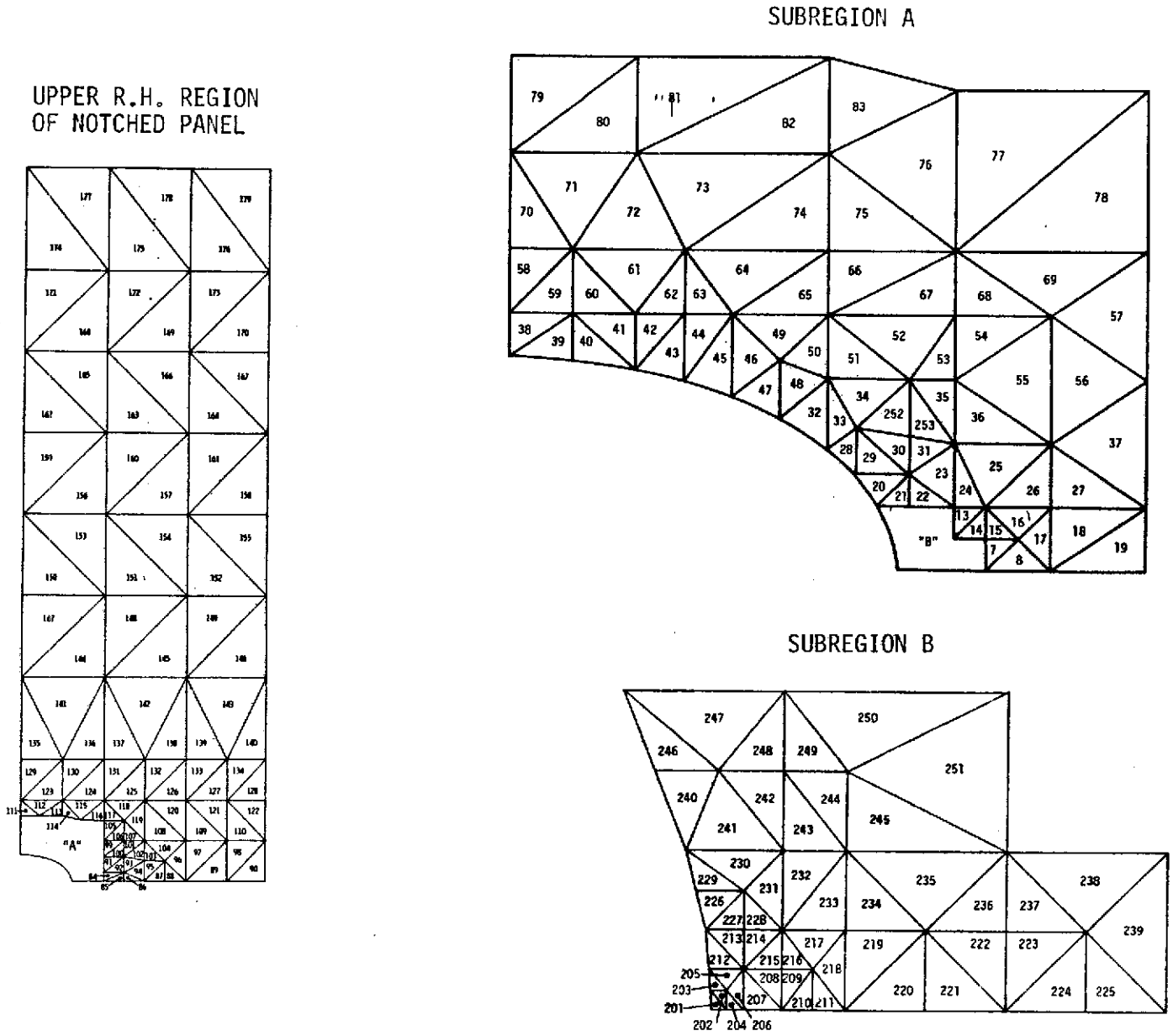

FIGURE 4.0-2: FINITE-ELEMENT MODEL NUMBER THREE SHOWING ELEMENT IDENTIFICATION NUMBERS

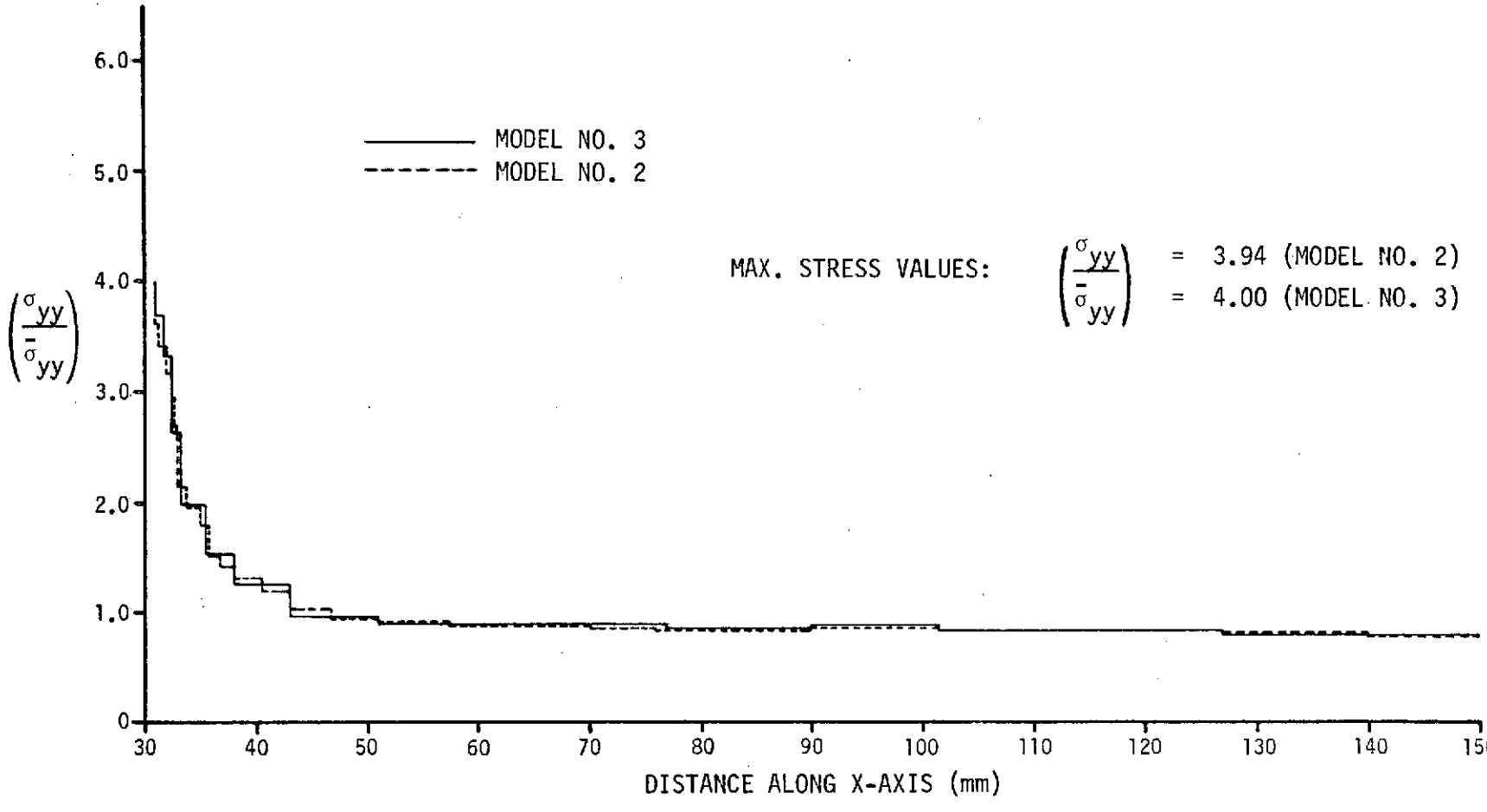

FIGURE 4.0-3: COMPARISON OF ELASTIC CHECKOUT CASES FOR FINITE-ELEMENT MODELS NUMBER 2 AND 3

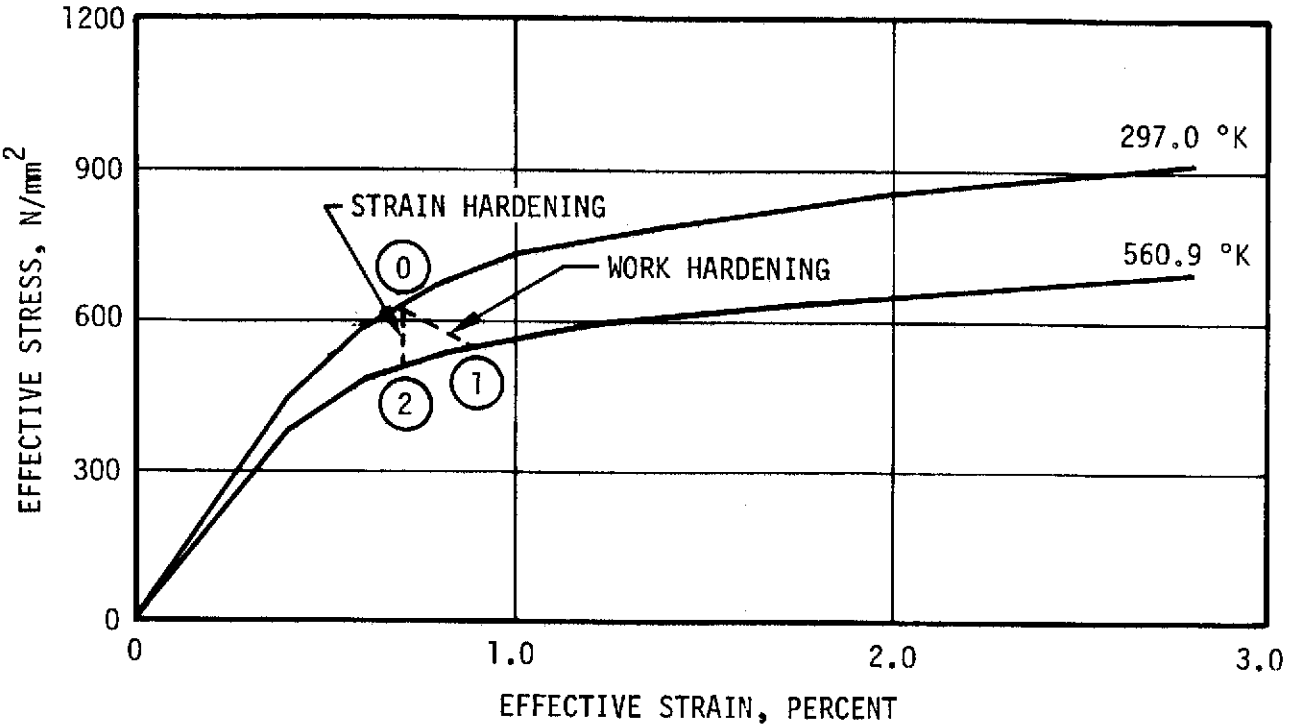

FIGURE 4.1-1: STRESS-STRAIN DATA USED IN BOPACE ANALYSIS

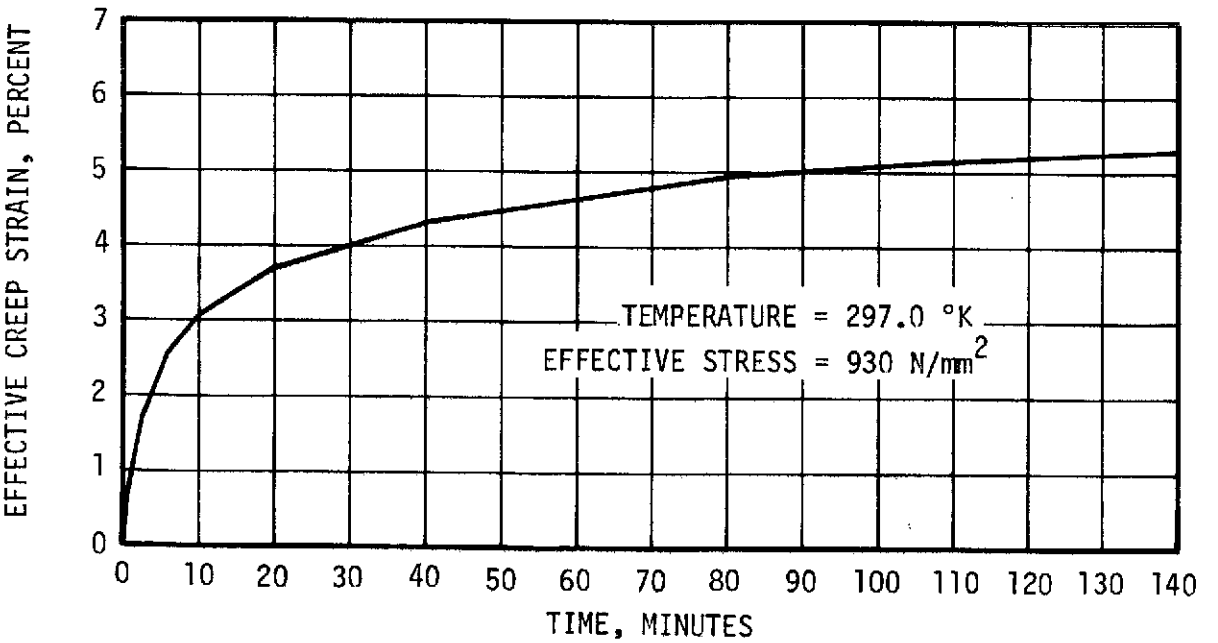

FIGURE 4.2-1: REFERENCE CREEP CURVE USED IN BOPACE ANALYSIS

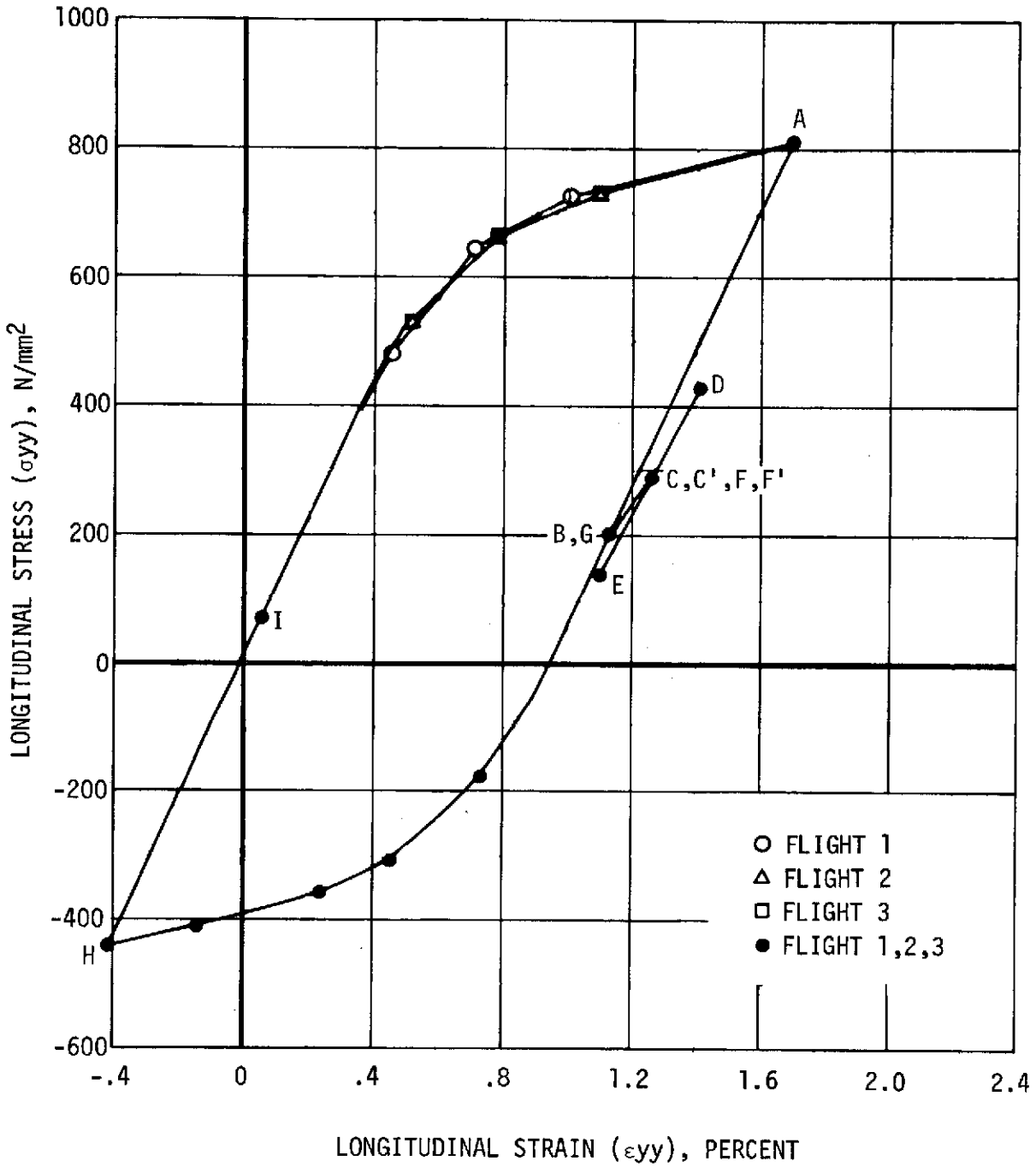

FIGURE 5.1-1: STRESS-STRAIN HYSTERESIS LOOP AT NOTCH (ELEMENT 201) - FLIGHTS 1, 2 AND 3.

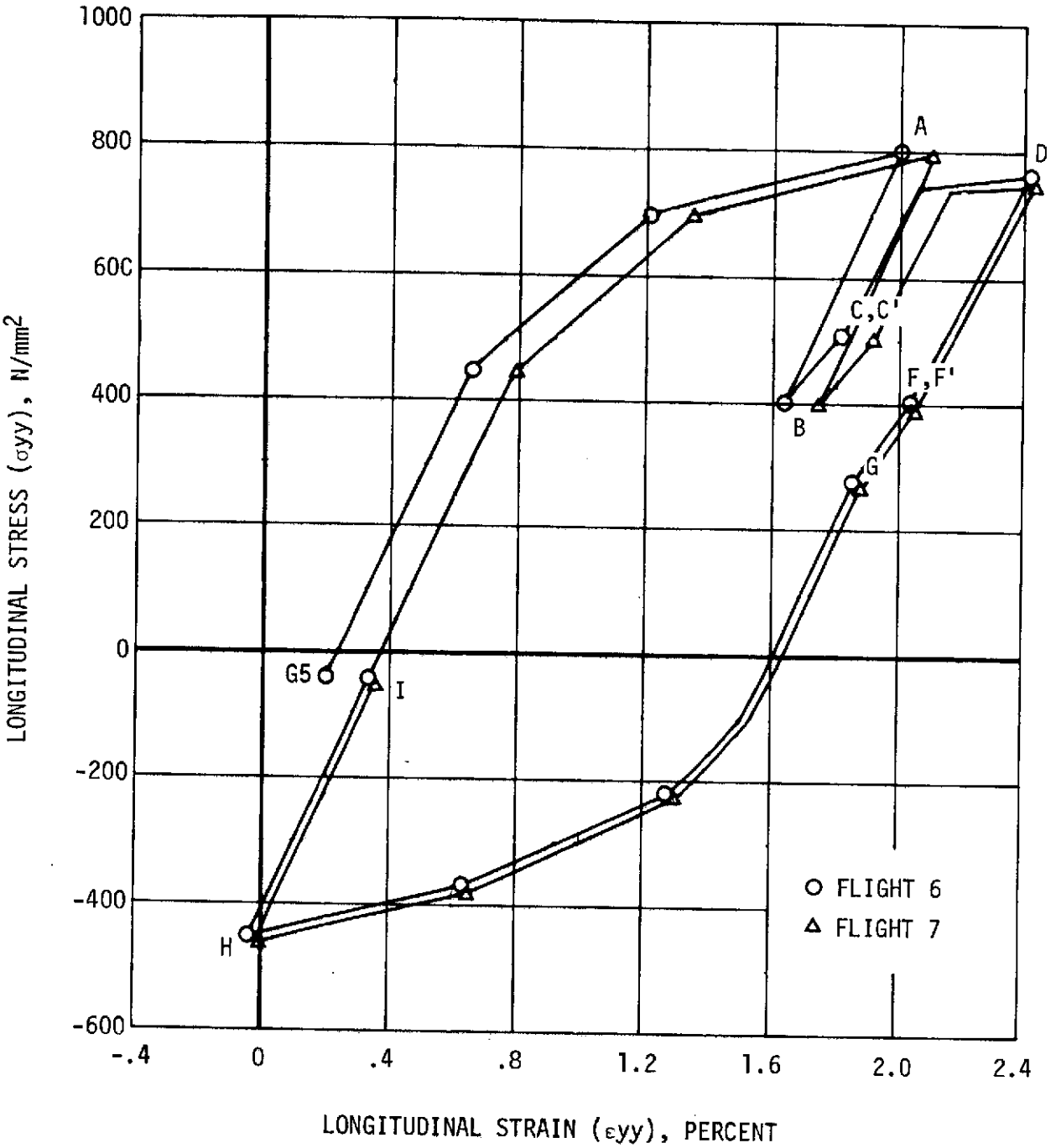

FIGURE 5.1-2: STRESS-STRAIN HYSTERESIS LOOPS AT NOTCH (ELEMENT 201) - FLIGHTS 6 AND 7

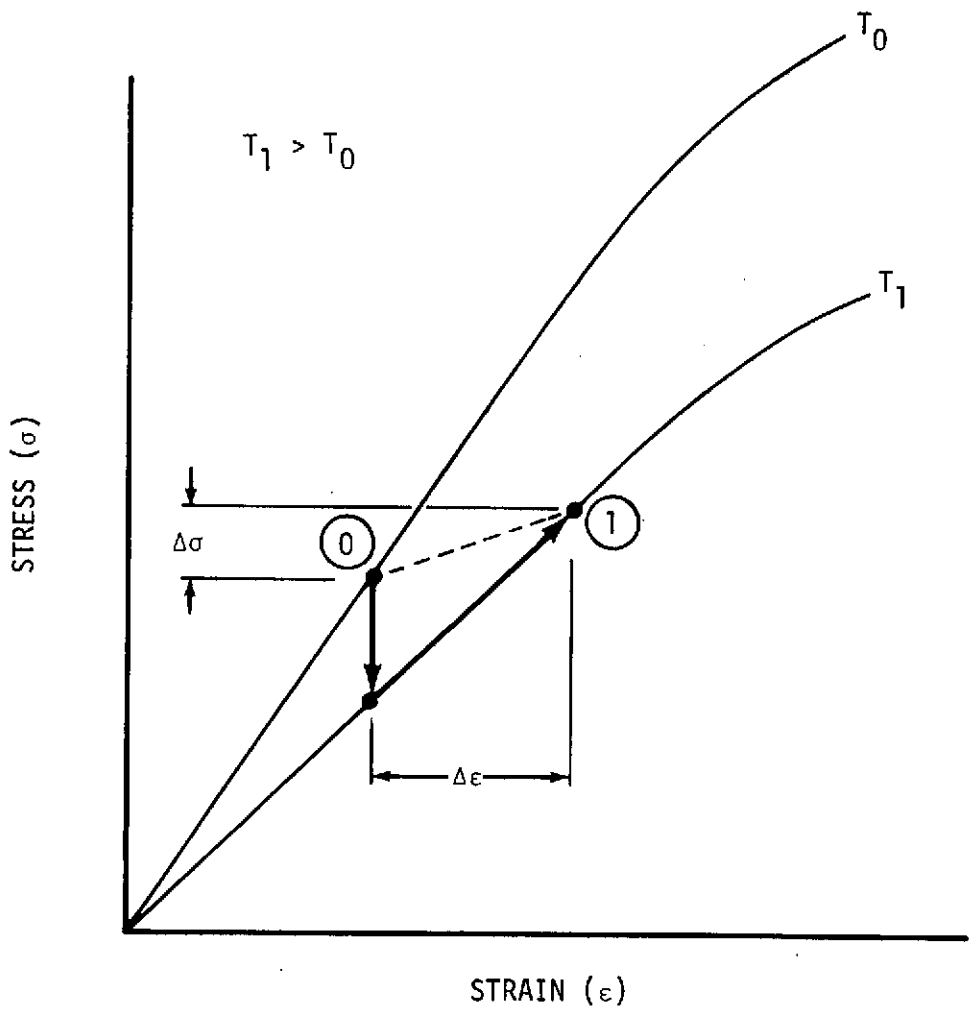

FIGURE 5.1-3: CHANGE IN ELASTIC STRESS AND STRAIN WITH CHANGE IN TEMPERATURE

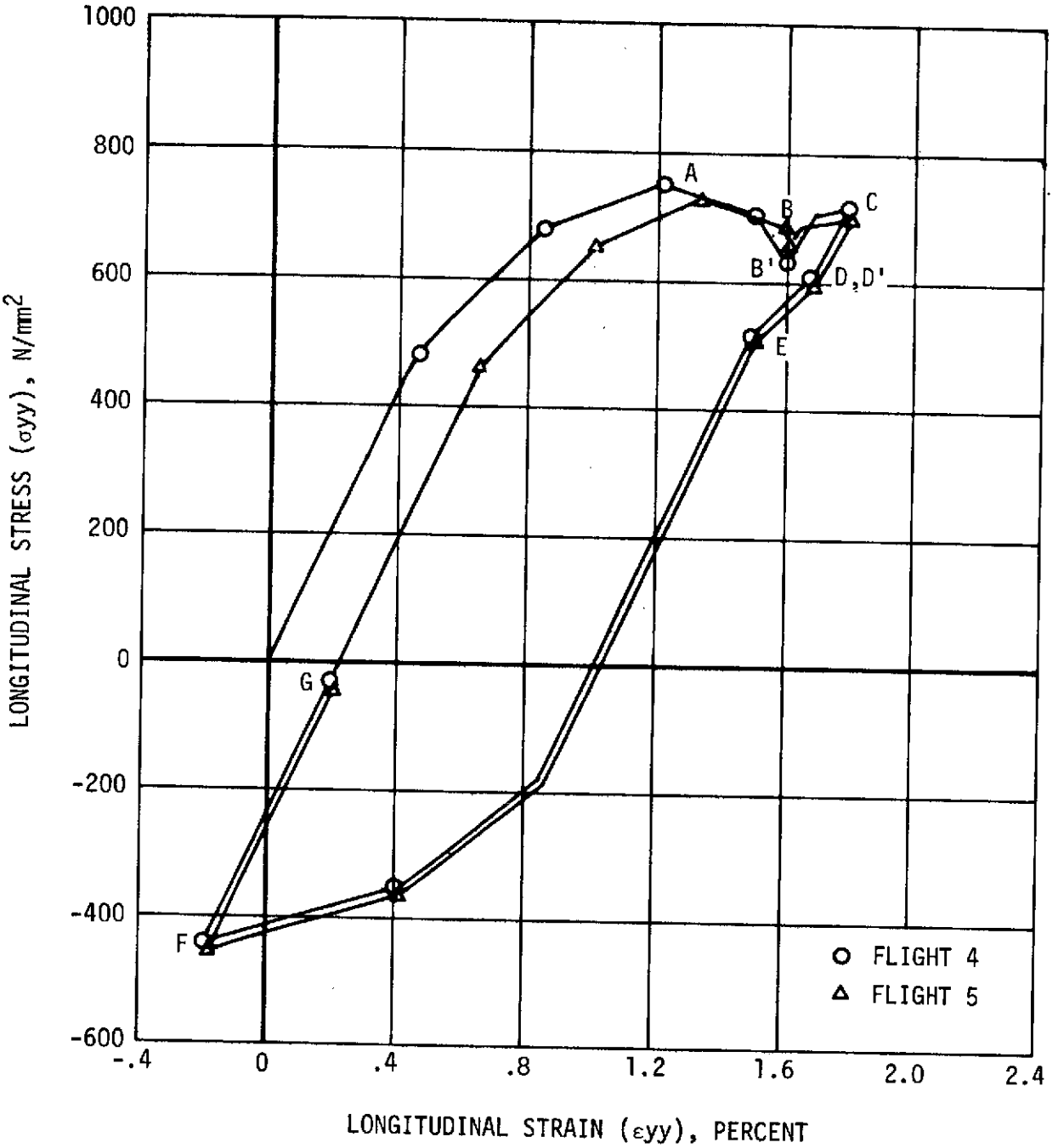

FIGURE 5.2-1: STRESS-STRAIN HYSTERESIS LOOPS AT NOTCH (ELEMENT 201) - FLIGHTS 4 AND 5

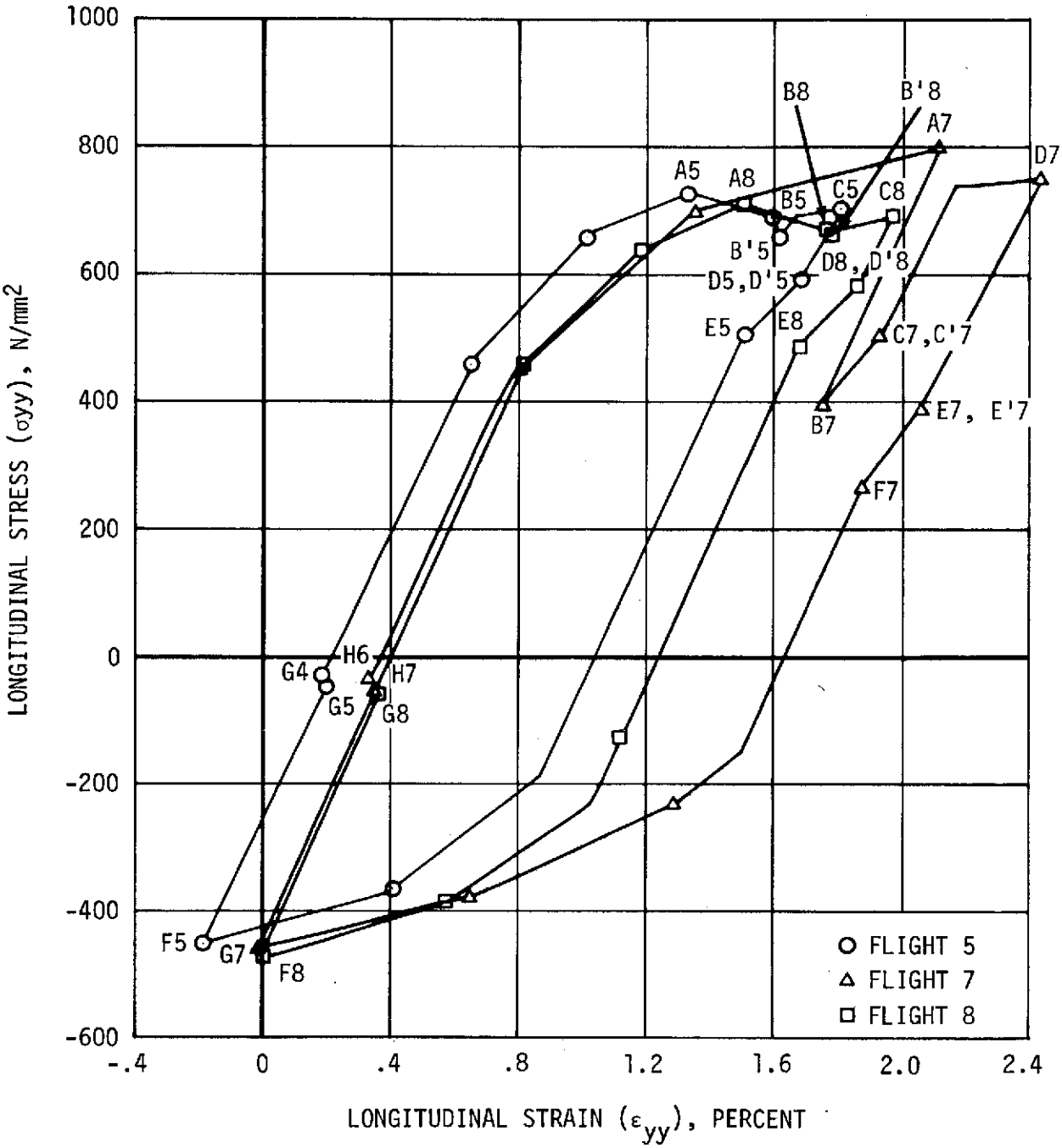

FIGURE 5.2-2: STRESS-STRAIN HYSTERESIS LOOPS AT NOTCH (ELEMENT 201) - FLIGHTS 5, 7 AND 8

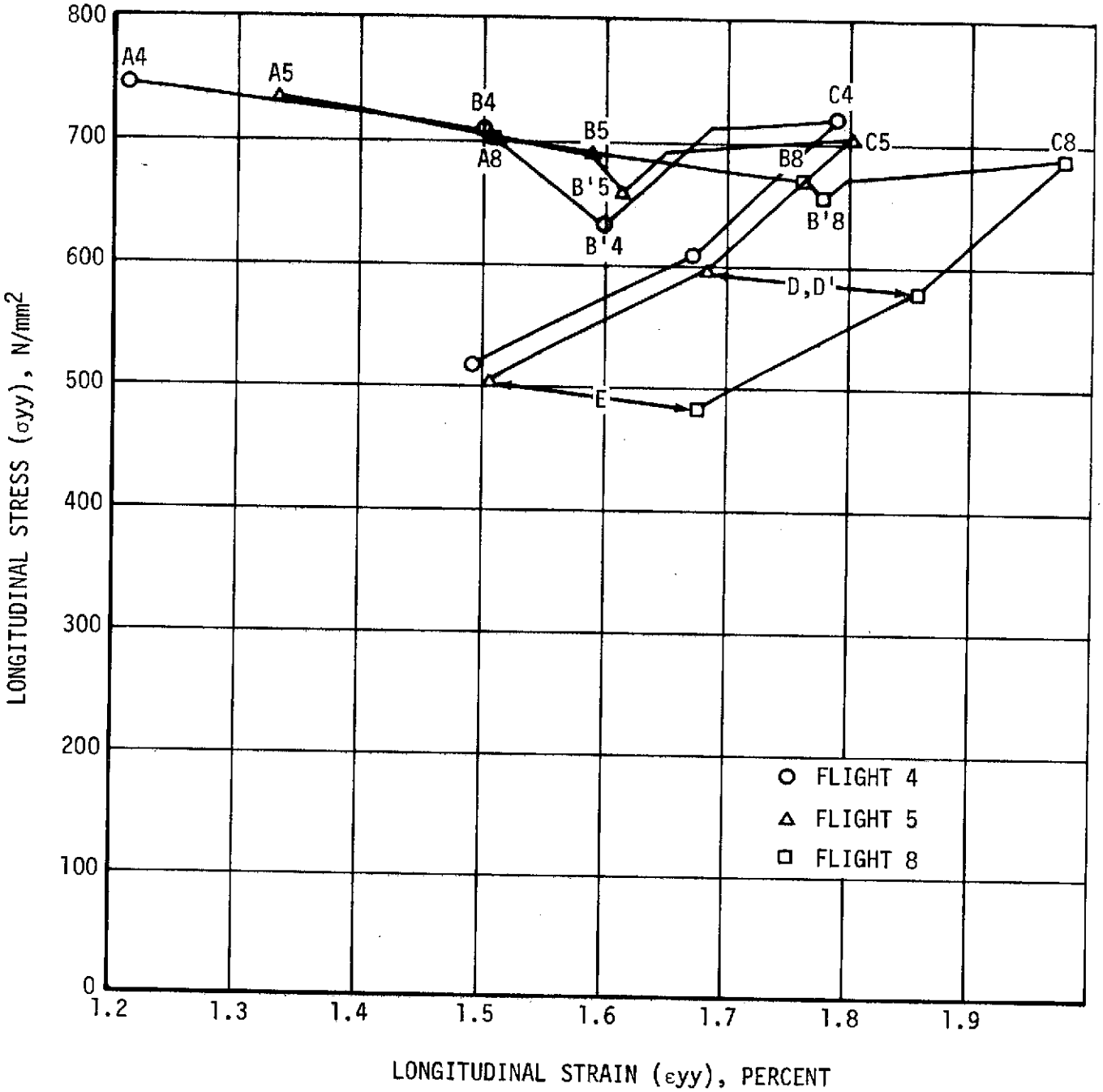

FIGURE 5.2-3: PORTION OF STRESS-STRAIN HYSTERESIS LOOPS EXHIBITING CREEP HARDENING AND VISCOELASTIC BEHAVIOR AT NOTCH (ELEMENT 201) - FLIGHTS 4, 5 AND 8

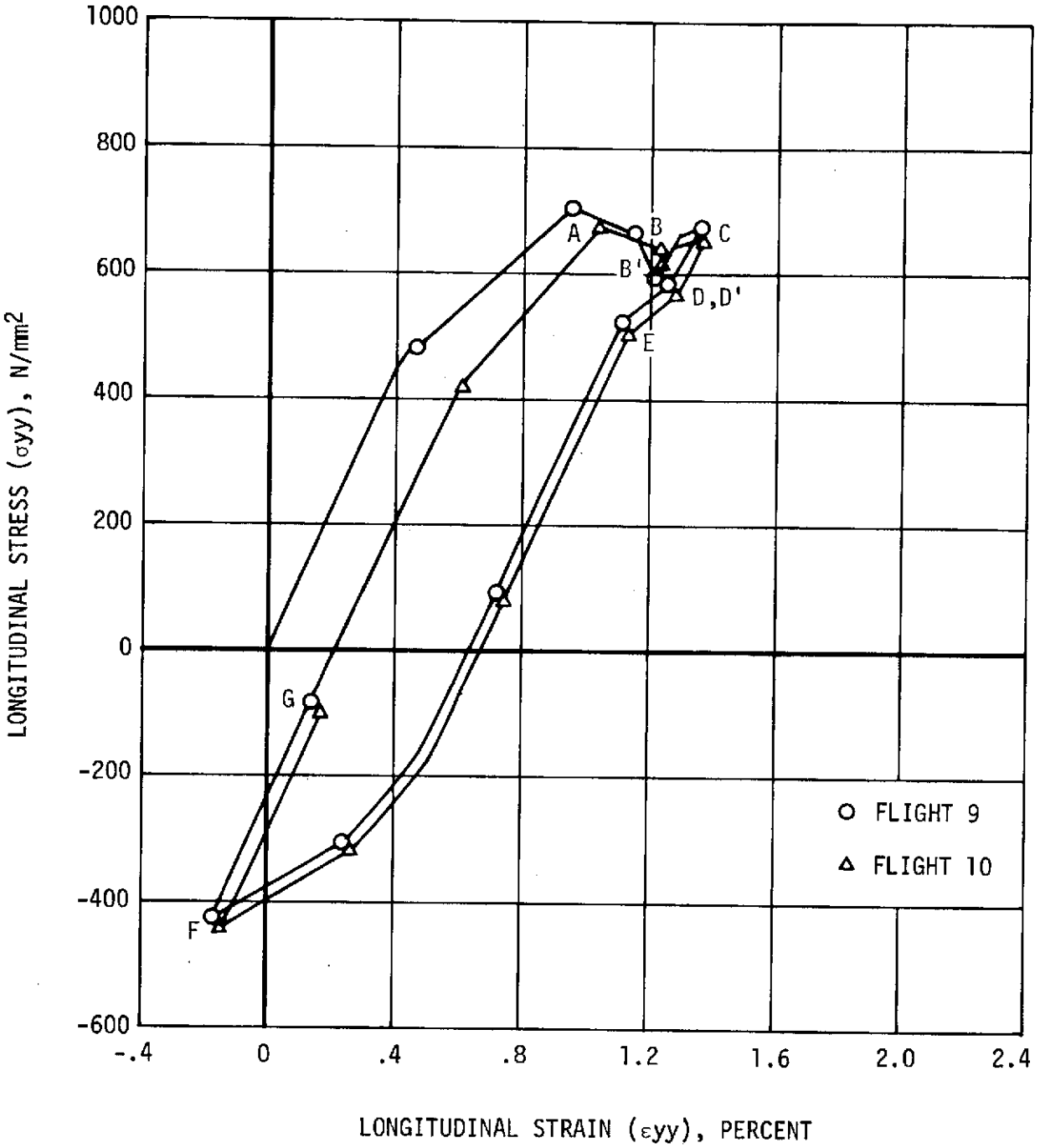

FIGURE 5.2-4: STRESS-STRAIN HYSTERESIS LOOPS AT NOTCH (ELEMENT 201) - FLIGHTS 9 AND 10

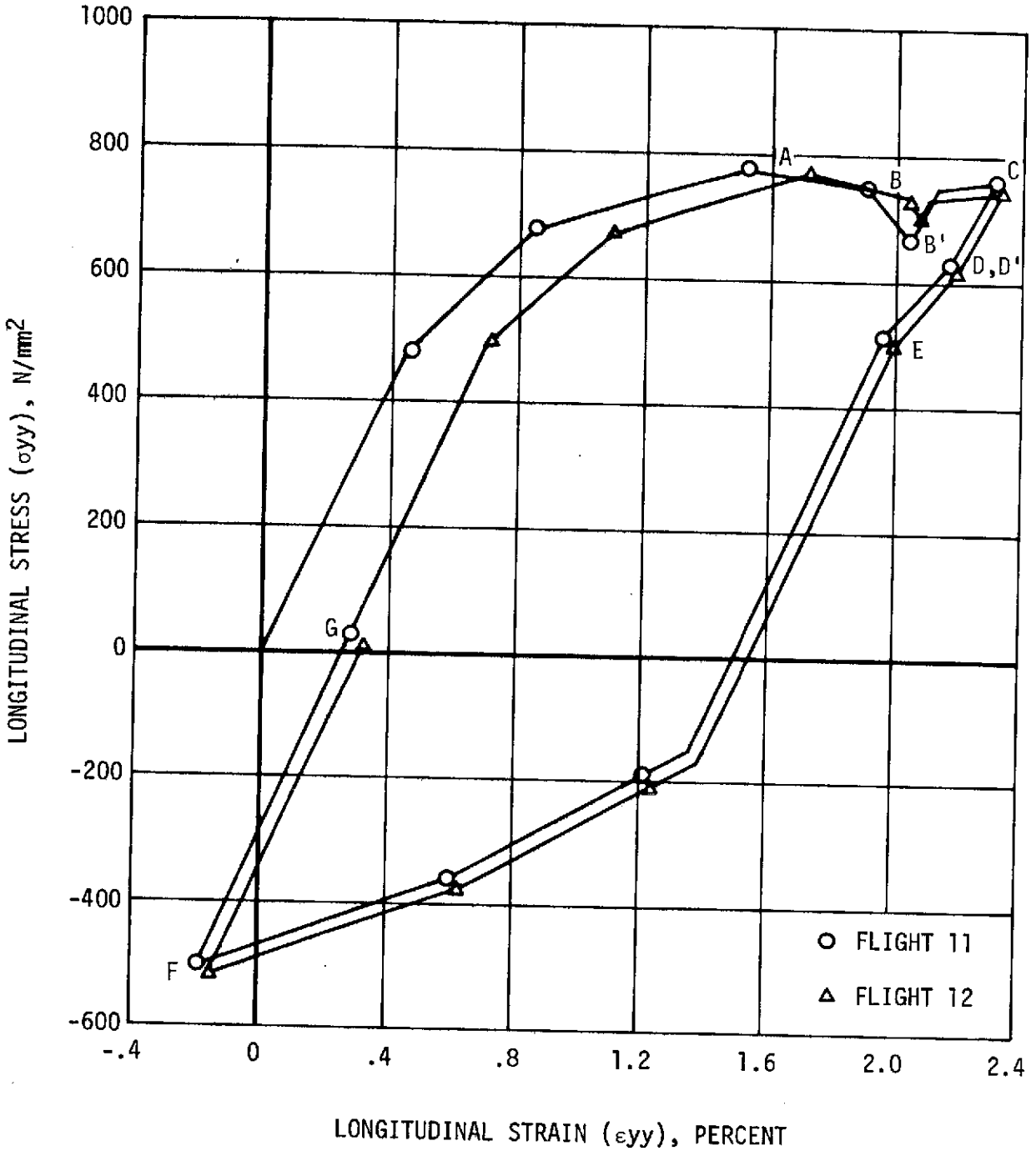

FIGURE 5.2-5: STRESS-STRAIN HYSTERESIS LOOPS AT NOTCH (ELEMENT 201) - FLIGHTS 11 AND 12

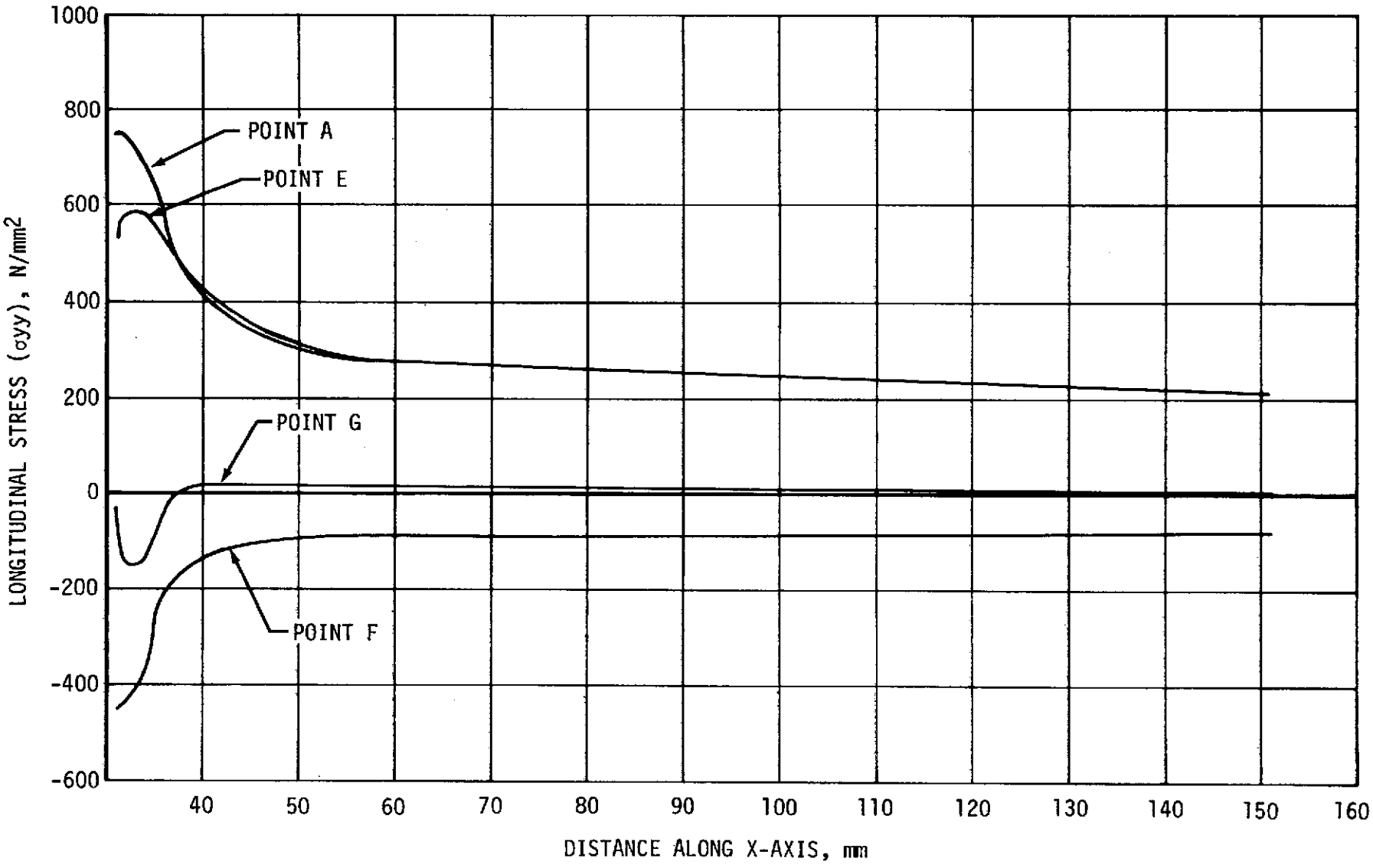

FIGURE 5.2-6: FLIGHT 4 - VARIATIONS IN LONGITUDINAL STRESS ALONG X-AXIS

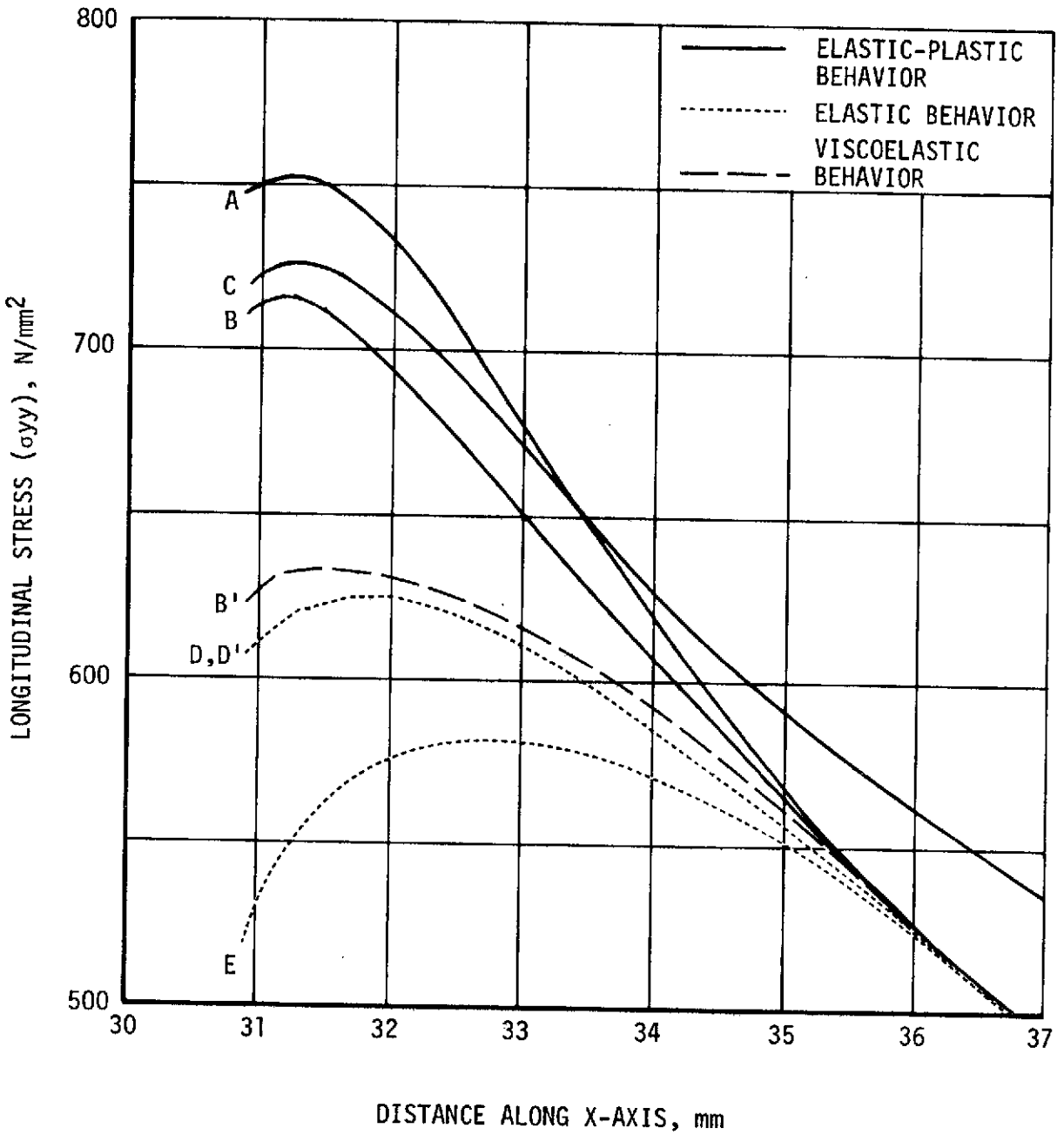

FIGURE 5.2-7: CURRENT MATERIAL BEHAVIOR AND VARIATION IN LONGITUDINAL STRESS IN VICINITY OF NOTCH AT y = 0 - FLIGHT 4

PROBLEM	FLIGHT NO'S. FOR EACH PROBLEM	KIND OF FLIGHT	DESIGN MEAN STRESS N/mm^2	TYPE OF STRESS SEQUENCE
I	1, 2, 3 (b)	BASIC	260	A (a)
II	4, 5 (c)	BASIC	210	C (a)
	6, 7 (d)	1000th	210	
	8 (c)	BASIC	210	
III	9, 10 (c)	BASIC	170	
IV	11, 12 (c)	BASIC	240	

NOMENCLATURE (Reference 2)

Basic Flight - Flight comprised of conditions expected to occur every operational flight.

1000th Flight - Flight comprised of conditions expected to occur every 1000th operational flight.

Operational Flight - Operational flying means the use of an airplane for routine commercial operation.

Design Mean Stress - Stress during level unaccelerated flight at maximum gross mass.

NOTES

a. See Figure 3.2-1
b. See Figure 3.2-2
c. See Figure 3.2-3
d. See Figure 3.2-4

TABLE 3.2-I: NOMENCLATURE AND RANGE OF PROBLEMS